THERMAL STRESS ANALYSIS ON DISC BRAKE ROTOR BY USING FINITE ELEMENT ANALYSIS

EE WEI XIANG

UNIVERSITI TEKNIKAL MALAYSIA MELAKA

THERMAL STRESS ANALYSIS ON DISC BRAKE ROTOR BY USING FINITE ELEMENT ANALYSIS

EE WEI XIANG

This report is submitted
in fulfillment of the requirement for the degree of
Bachelor of Mechanical Engineering with Honors

Faculty of Mechanical Engineering

UNIVERSITI TEKNIKAL MALAYSIA MELAKA

2019

DECLARATION

I declare that this project report entitled "Thermal Stress Analysis of Disc Brake Rotor by using Finite Element Analysis" is the result of my own work except as cited in the references.

Signature : ……………………….

Name : Ee Wei Xiang

Date : ……………………….

SUPERVISOR DECLARATION

I hereby declare that I have read this project report and in my opinion this report is sufficient in terms of scope and quality for the award of the degree of Bachelor of Mechanical Engineering.

Signature : ………………………….

Name : Dr. Mohd Zaid Bin Akop

Date : ………………………….

ABSTRACT

In today automotive industries, braking system is an essential component of the vehicle. Typically, there are two type of braking system, which is disc brake and drum brake. In order to achieve a better braking performance in a shorter distance, disc brake is installed on the front wheel and drum brake is installed on the rear wheel. This is because the disc brake can dissipate the heat efficiently compared to the drum brake. Therefore, thermal management is an important factor that can affect the performance of braking system. In this project, four design specification of disc brake rotor is used to analyze the thermal stress distribution. Gray cast iron is selected as the material of disc brake rotor in ANSYS. The convective heat transfer coefficient for certain surface of rotor that exposed to air directly is applied. FEA software is used to determine the thermal stress of four design specification of disc brake rotor. The result of four different design specification of disc brake rotor is compared after simulation process is completed. The slotted rotor shows a lower temperature in steady state thermal analysis and transient thermal analysis. Furthermore, slotted rotor shows a lower deformation and moderate equivalent (Von-Mises) stress in static structure analysis and transient structure analysis.

ABSTRAK

Pada hari ini industri automotif, sistem brek adalah komponen utama kenderaan. Biasanya, terdapat dua jenis sistem brek, iaitu brek cakera dan brek dram. Untuk mencapai prestasi brek yang lebih baik dalam jarak yang lebih pendek, brek cakera dipasang pada roda depan dan brek drum dipasang pada roda belakang. Ini kerana brek cakera boleh menghilangkan haba dengan cekap berbanding brek dram. Oleh itu, pengurusan haba merupakan faktor penting yang boleh menjejaskan prestasi sistem brek. Dalam projek ini, empat spesifikasi reka bentuk cakera brek cakera digunakan untuk menganalisis taburan tekanan haba. Tuang besi kelabu dipilih sebagai bahan pemutar brek cakera di ANSYS. Pekali pemindahan haba konveksi untuk permukaan pemutar tertentu yang terdedah kepada udara terus digunakan. Perisian FEA digunakan untuk menentukan tekanan haba empat spesifikasi reka bentuk cakera brek cakera. Hasil daripada empat spesifikasi reka bentuk rotor brek cakera yang berbeza akan dibandingkan selepas proses simulasi diselesaikan. Pemutar slotted menunjukkan suhu yang lebih rendah dalam analisis haba keadaan mantap dan analisis termal sementara. Tambahan pula, pemutar slotted memperlihatkan tekanan ubah bentuk yang rendah dan tegasan sederhana (Von-Mises) dalam analisis struktur statik dan analisis struktur sementara.

ACKNOWLEDGEMENT

First and foremost, I would like takes this opportunity to express my sincere gratitude to my supervisor, Dr. Mohd Zaid Bin Akop for his invaluable guidance and continuous encouragement in making this project successful. I really appreciated about the continuous guidance from beginning to the end of this project. Some people say, Shi En mountain, because mountains Wei Wei, revered. I would also like to say, Shi En like the sea, because the sea is vast, beyond measure. I also want to say thank you to my BMCG friends who helping me to complete this project, sharing knowledge with me, and solving problem for me. Finally, I am grateful to my parent who support me in term of mental and physical.

TABLE OF CONTENTS

LIST OF FIGURES

LIST OF TABLES

LIST OF ABBREVIATIONS & SYMBOLS

3D	Three dimensional
FEA	Finite element analysis
Q	Rate of heat transfer
m	Mass
C	Specific heat capacity
ΔT	Temperature difference
J	Joule
σ	Stefan-Boltzmann constant
x	Distance
k	Thermal conductivity
ε	coefficient of emissivity
T_S	Surface temperature
T_∞	Ambient temperature
h	Convective heat transfer coefficient

CHAPTER 1

INTRODUCTION

1.1 Background of Research

In order for a car to have a safe trip, brakes, tires, and steering system is the most important safety feature. This is because the accident can be prevented by changing the speed and direction of the car. A continuous adjustment of speed and direction is required for user to drive with different traffic conditions such as slippery, wet, and dry road. The main function of the disc brake is to slow the vehicle, maintain vehicle speed during downhill operation, and hold the vehicle stationary on a grade. During braking condition, the kinetic and potential energy of the vehicle is transforms to the thermal energy by frictional force that generate between brake pad and rotor. Once the user presses the brake pedal, a large amount of heat will be generated between the brake pad and rotor to opposite the torque of the wheel. Therefore, heat management on the rotor is an important factor that need to predict and control for the reason of economic and safety feature. A high temperature that exists may lead to the brake fade and cause the accident to occur. The heat energy can be dissipated through the conduction, convection, and radiation. In this project, the result of thermal stress analysis of four different design will be compared after several braking operation.

1.2 Problem Statement

There are several factors that can affect the performance of braking system during the braking condition. For example, pressure, coefficient of friction, frictional contact surface, and rate of heat dissipation. Among those factors, the rate of heat dissipation is the main factor that can affect the braking system significantly (Satope, 2017). Since the area of convection that take places between the air and rotor can affect the rate of heat dissipation, a ventilated disc brake rotor with different design which may affect the rate of heat dissipation is selected as the title of research. The temperature and deformation of disc brake after several times of braking are determined by the ANSYS. Theoretically, the bigger size or area of drilling will increase the rate of heat dissipation and increase the performance of braking system. However, the strength of the disc brake rotor may be reduced due to the drilled hole and slotted area. Therefore, it is important to study and compare the result of thermal stress distribution on these four types of disc brake rotor.

1.3 Objective

The objectives of this project are as follows:

1. To study the thermal stress distribution in disc brake rotor on vehicle caused by temperature rise after several braking operation of vehicle.
2. To analyse the effect of design of disc brake rotor on the cooling performance and deformation after several braking operation of vehicle.
3 To compare the effect of design of disc brake rotor on the cooling performance and deformation after several braking operation of vehicle.

1.4 Scope of Project

The scopes of this project are:

1. Design 3D model of 4 different design specification of disc brake rotor.
2. Mesh the model.
3. Finite element analysis (ANSYS) will be used to analyze different design specification of disc brake rotor.
4. Compare the result of thermal stress analysis of different design of disc brake rotor.

1.5 General Methodology

The actions that need to be carried out to achieve the objectives in this project are listed below.

1. Literature review

   Journals, articles, or any materials regarding the project will be reviewed.

2. Drawing

   Different design of disc brake rotor will be drawn in SolidWorks software.

3. Simulation

   Simulation of the 3D model will be done using the ANSYS software.

4. Analysis and Comparison

   Analysis and comparison of the rate of heat dissipation will be calculated. Result will be proposed based on the analysis.

5. Report writing

   A report on this study will be written at the end of the project.

CHAPTER 2

LITERATURE REVIEW

2.1 Trends of Industry

Both of the disc brake and drum brake system are based on a hydraulic pressure system. In today automotive technology, a disc brake is commonly found on the front wheel as well as rear wheel especially in the modern car such as Mercedes-Benz and BMW. It is attached to the rotating wheel by using the wheel hub. The disc brake rotor can be solid or vented, but the vented rotor has a better efficiency compared to solid rotor due to it has a larger surface to dissipate the heat more easily (*Complete Guide to Disc Brakes and Drum Brakes - Les Schwab*, no date). Figure 2.1 shows the solid rotor and vented rotor.

Figure 2.1: Solid rotor and vented rotor

(Source: www.lesschwab.com)

Although the use of disc brake on all four wheels become more and more popular across the century especially in heavier vehicle, but a drum brake still uses for the rear wheel of some model of car due to the cost factor. The inertia cost of the drum brake is lower than the disc brake (*Automotive Mechanics,2E - S. Srinivasan - Google book*. 2nd Edition, 2003). Furthermore, the weight factor become an important factor to install the disc brake on the front wheel. The weight of drum brake is heavier about twenty percent than disc brake (*Automotive Mechanics,2E - S. Srinivasan - Google book*. 2nd Edition, 2003). Typically, an unloaded vehicle is already about ten percent heavier in front due to the engine is located in front of car (*Complete Guide to Disc Brakes and Drum Brakes - Les Schwab*, n.d.). Once the user presses the brake pedal, the weight of the car will transfer to the front first due to the motion and inertia of the car. According to the Newton's first law, inertia is the resistance of any physical object to any change in its velocity. So, more braking power is needed for the front wheel to stop the vehicle immediately. A disc brake can provide more stopping power and a shorter stopping distance compared to drum brake. Figure 2.2 shows the important of disc brake on front wheel.

Figure 2.2: Important of disc brake on front wheel

(Source: www.6thgearautomotive.com)

In order to achieve the safety criterion, heat management on the braking system is very important. It can ensure the braking performance is consistent across the life time. This is because overheat of friction material will cause the loss of stopping power and leading to brake fade (Belhocine *et. al*, 2016). Due to the disc brake is exposed to air directly, it can transfer the heat through conduction, convection, and radiation while for drum brake, it can only transfer the heat through the conduction because the drum brake components are not exposed to the air (*Complete Guide to Disc Brakes and Drum Brakes - Les Schwab*, n.d.). Therefore, the disc brake rotor has a better heat dissipation and consistency compared to drum brake. Figure 2.3 shows the structure of disc brake and drum brake.

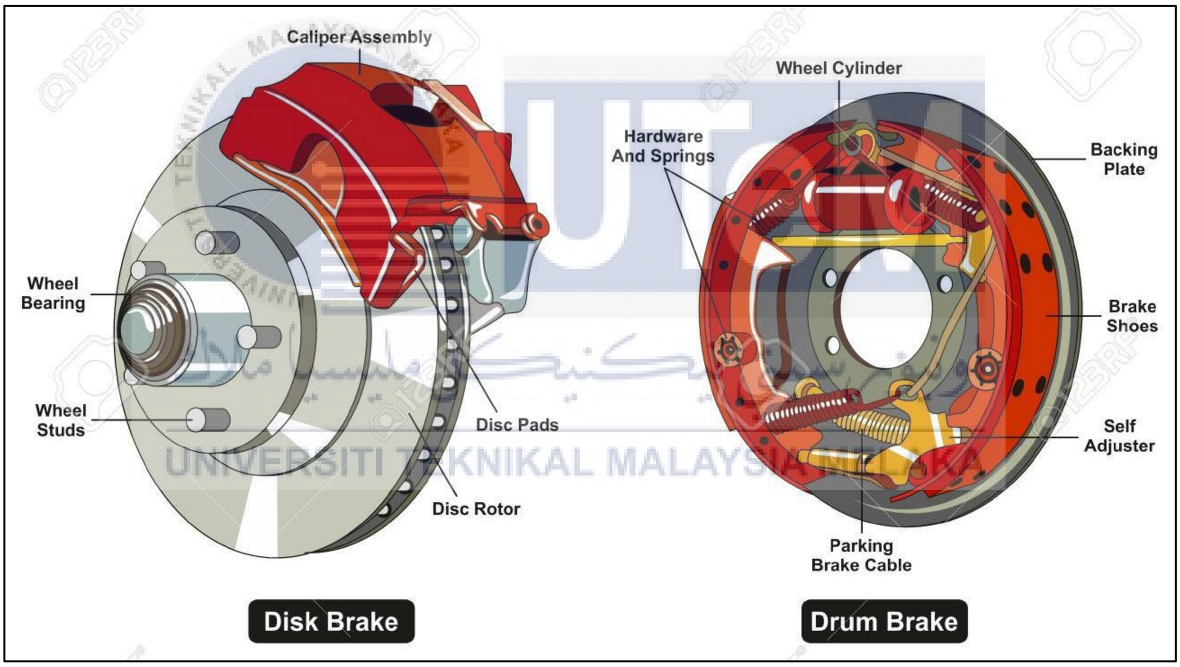

Figure 2.3: Structure of disc brake and drum brake

(Source: es.123rf.com)

2.2 Working Principle

The disc brake is a type of brake that use the caliper to sequence the brake pads to stop or control the speed of the car. Typically, the disc brake is located at the front wheel and drum brake is located at the rear wheel of the vehicle. The reason is that, the disc brake rotor has a better heat dissipation and a greater resistance to fading after a long-time operation.

Basically, there are five major parts inside the hydraulic brake system, which is brake pedal, pushrod, master cylinder assembly, reinforced hydraulic lines, and brake caliper assembly. The hydraulic brakes system usually is filled with glycol-ether based brake fluid to complete the braking operation. This is because the glycol-ether based of brake fluid has a high boiling point to prevent the vaporization and a better heat dissipation to maintain the performance of hydraulic brake system.

Once the user presses the brake pedal, the master cylinder piston will pressurize the brake fluid. After that, the brake fluid will flow from brake fluid reservoir into the hydraulic lines and push the left piston and right piston toward the rotor to generate a torque that will opposite the direction of wheel and reduce the speed of the wheel. This action will generate a friction force on the rotor and transform the potential energy and kinetic energy of the car into thermal energy. Figure 2.4 shows the hydraulic brake system of disc brake system.

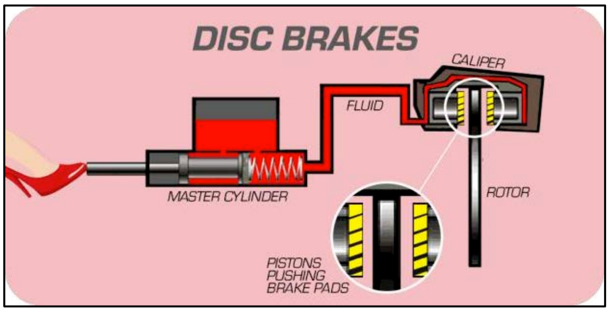

Figure 2.4: Hydraulic brake system of disc brake system

(Source: yourbrakes.com)

2.3 Type of Disc Brake Rotor

2.3.1 Material

Material selection is an important factor that can affect the heat dissipation. This is because each material has different physical, chemical, and mechanical properties. In order to select a suitable material, many factors need to be taken into the consideration, including level of environmental impact, design suitability, cost, source of its components, and type of manufacturing process (Ogunkah and Yang, 2012).

Vikas *et. al* (2016) present a paper on Comparative Analysis of Disc Brake Model for Different Materials Investigated under Tragic Situations. Four main types of material are selected as the material of disc brake which is mild steel, cast iron, aluminum alloy, and ceramic. Among those material, cast iron has a moderate cooling performance compared to other material. Ceramic has a highest rate of heat dissipation among those material after a certain time, but it is costly than other material. Thus, ceramic only use in sensitive application such as defense, aircrafts, and racing cars (Gupta *et. al.*, 2016). Table 2.1 shows the temperature of disc brake for different material at various time intervals.

Table 2.1: Temperature of disc brake for different material at various time intervals

(Source: Gupta *et al.*, 2016)

Time in seconds	1.2 *s*	1.8 *s*	10 *s*
Material	**Temperature in *K***		
Mild steel	575.6	558	392.7
Cast iron	617.4	593.2	415.7
Aluminum alloy	569.2	564.4	448.1
Ceramic AL2O3 (99.5%)	788.9	749.8	471.3

Therefore, cast iron is the best choice for disc brake in today automotive technology because of its strength and thermal properties, high temperature resistance and availability (Amrish, 2016). In this project, cast iron is selected as the material of 3D modeling and FEA. Table 2.2 shows the properties of cast iron.

Table 2.2: Properties of cast iron

(Source: Amrish, 2016)

Density (kg/m^3)	7200
Thermal Conductivity (W/m-K)	54.5
Specific Heat (J/kg-K)	586
Coefficient of friction	0.25

2.3.2 Design Specification

In order to increase the heat dissipation through convection, several types of design are used in today automotive technology. Since the area of convection that take places between the air and rotor can affect the rate of heat dissipation, a ventilated disc brake rotor with different design which may affect the rate of heat dissipation is selected. Figure 2.5 shows the design of disc brake rotor. Table 2.3 below shows the design specification.

Figure 2.5: Design of disc brake rotor

(Sources: r1concepts.com)

Table 2.3: Design specification

(Source: www.r1concepts.com)

Design	Specification
Blank and smooth	A smooth or plain surface, with no holes or marking in the metal.
Drilled	A series of holes drilled into the metal.
Slotted	Several slots on the surface
Slotted and drilled	A combination of slotted and drilled.

2.4 Type of Brake Pad

2.4.1 Material

Brake pads is an important component that use to create friction on disc brake rotor. By pressurized the brake fluid, the two brake pads that installed on brake caliper will move toward the rotor and generate a large friction force that can overcome the torque and stop or slow down the vehicle immediately. The friction generated between brake pad and rotor depend on the power and weight of vehicle. The larger the weight and power of the vehicle, the larger the frictional force. Therefore, the brake pad will undergo an extremely stress during the braking condition especially for a loaded vehicle because it is a tool that apply the pressure to the rotor. In today automotive technology, three main type of brake pad are selected as the material of brake pad which is non-metallic or organic, semi-metallic, and ceramic (Azuma, 2018).

Non-metallic or organic is the softest brake pad. This type of brake pad is the combination of rubbers, glasses, and high temperature resins. Due to the softest characteristics, it creates less noise among those material. However, it is a dust producer during braking condition because it deteriorate faster.

Semi-metallic is the most common material that use by many different vehicles. This is made by copper or graphite, wool or steel wire, and friction modifiers. It has a better heat dissipation and can last longer over a certain period due to it contain 30 % - 65 % of metal in this brake pad. At the same time, it produces more noise and wear down the rotor faster compare to non-metallic brake pad. Moreover, one of the disadvantages of this brake pad is it has a lower performance or lower braking power during low ambient temperature.

For ceramic brake pad, it has a highest price among those brake pad. This type of brake pad is made by bonding agents, ceramic fibers, and nonferrous filler materials. It usually found in high performance vehicle, because it can absorb the high temperature generated by high speed and frequency braking. Besides that, it produces less noise and dust during the braking condition.

2.5 Heat

2.5.1 Introduction

Heat is a useful energy in the world. Heat is thermal energy that flow from a higher temperature object to a lower temperature object. According to Zeroth law of thermodynamic, heat cannot transfer between two objects in thermal equilibrium which has no difference in temperature. Temperature is a measurement of average kinetic energy of atom and molecule. It has a symbol of Q and unit of J. The amount of heat energy released or absorbed can be calculate using the Eq. (2.1) where m is the mass of substance, c is the specific heat capacity, and ΔT is the temperature difference.

$$Q = m \times C \times \Delta T \tag{2.1}$$

Heat energy can transfer with media or without media through conduction, convection, and radiation due to temperature difference. Heat will dissipate by conduction through the brake assembly and wheel hub, convection to the surrounding air and radiation to the nearby component (Macužić *et al.*, 2015). Figure 2.6 shows the way of heat dissipate from disc brake rotor.

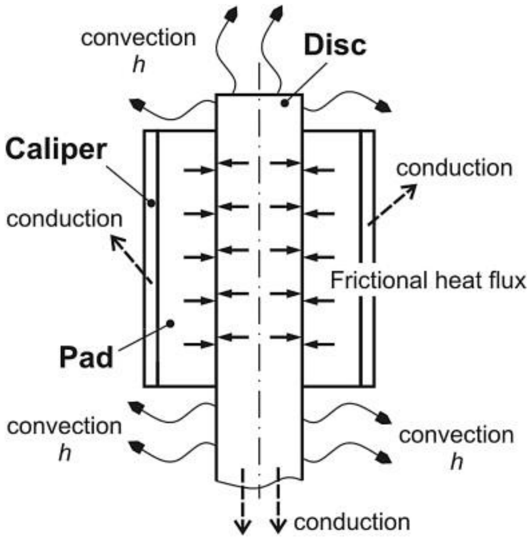

Figure 2.6: Way of heat dissipate from disc brake rotor

(Source: Deshpande and Kamat, 2017)

2.5.2 Conduction

Conduction take place when the two solid object is in direct contact condition. Heat transfer from the hot object to the cool object due to temperature difference. In this case, heat is conducted to the hub and wheel assembly (Voller, 2003). Although conduction is an effective way to dissipate heat, but it may lead to negative impact such as brake fluid vaporization, damaged seals, and wheel bearing damage. The governing equation for conduction is called as Fourier's law and it is shows in Eq. (2.2):

$$Q = -kA\frac{\partial T}{\partial x} \tag{2.2}$$

Where Q is the heat flux perpendicular to the surface of area, [W]; A is the surface area of heat flows occur, [m^2]; k is the thermal conductivity, [$Wm^{-1}K^{-1}$]; ∂T is the temperature difference [K]; and ∂x is the perpendicular distance to the surface traveled by the heat flux [m].

2.5.3 Radiation

Heat transfer through the empty space that have a certain distance without molecule is called as radiation. Radiation is the product of wavelength and frequency, it travels at the speed of light. Heat can dissipate by radiation to the ambient and adjacent surface. The amount of heat dissipate by radiation is calculate by the Eq. (2.3), where A is area emitting radiation, T_D is surface temperature, T_∞ is the ambient temperature.

$$Q_{rad} = \sigma \varepsilon A_{rad} \left(T_S{}^4 - T_\infty{}^4\right) \tag{2.3}$$

Where ε is the coefficient of emissivity [=1 for ideal radiator]; σ is the Stefan-Boltzmann constant of proportionality [5.669×10^{-8} Wm^{-2} K^{-4}]; A is the radiating surface area [m^2]; T_S is the absolute temperature of surface [K]; and T_∞ is the ambient temperature [K].

2.5.4 Convection

The transfer of heat between the fluid is called as convection. The fluid can be liquid or gases. Once the fluid is heated from the hot reservoir, the hot fluid at a system will become less dense and it will move upward while cool fluid that has a higher density at this time will move downward. This repeating process created a convection current that increase the temperature of the fluid in a system. The equation that use to calculate the amount of heat dissipate is shows as Eq. (2.4).

$$Q = hA(T_s - T_\infty) \tag{2.4}$$

Where h is the convective heat transfer coefficient [$Wm^{-2}K^{-1}$]; T_∞ is the ambient temperature; and T_s is the temperature of the surface.

Voller (2003) present a paper on Analysis of Heat Dissipation from Railway and Automotive Friction Brakes. Once of the main objective in this research is to compare the different mode of heat dissipation. The study shows that the amount of heat dissipate by convection is directly proportional to the rotational speed at high temperature and low temperature of friction surface. The radiation and conduction are speed independent, but the ratio of each mode of heat dissipation change with speed. Figure 2.7 shows that the result obtains by Voller when the surface temperature is at 600 °C. Table 2.4 shows the result that obtained by Voller.

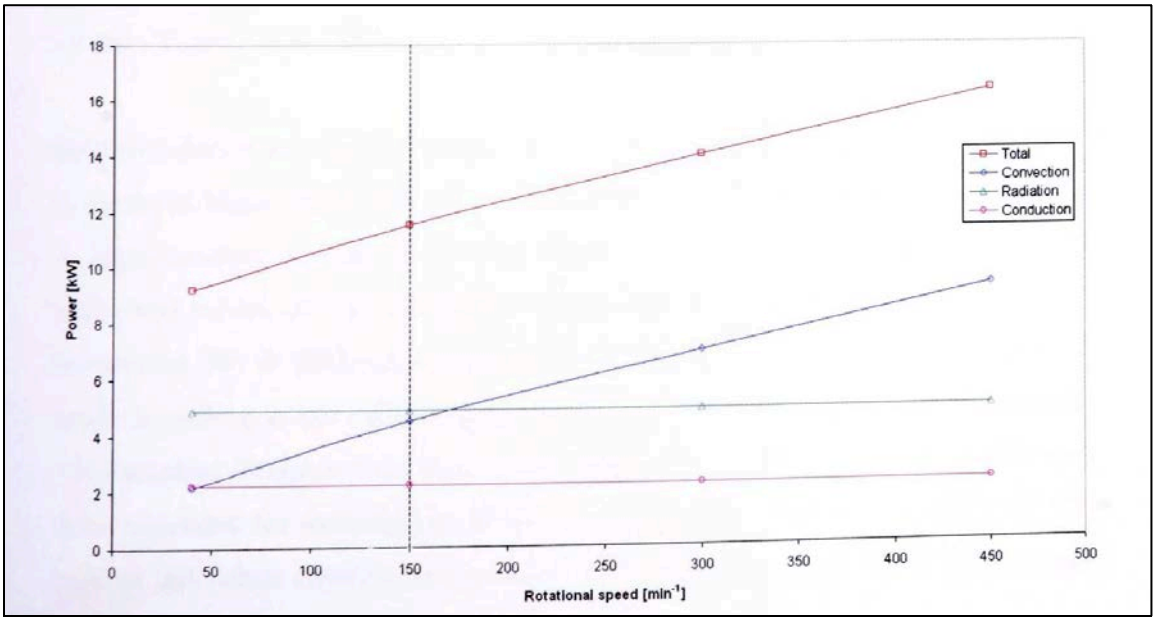

Figure 2.7: Contribution of each mode of heat transfer at 600 ℃

(Sources: Voller, 2003)

Table 2.4: Result of heat dissipate by convection at different speed

(Source: Voller, 2003)

Temperature of friction surface (℃)	600	
Speed (*km/h*)	8	90
Percentage of heat dissipate by convection (%)	18	57

2.6 Finite Element Analysis (FEA)

2.6.1 Introduction

For human to understand the physical phenomena, mathematics equation such as partial differential equation is used to solve the problem. The partial differential equation can used to describe the physical phenomena such as thermal transport, structural or fluid behavior, wave propagation, the growth of biological cells, etc. For a computer to solve the partial differential equation, a numerical technique, FEA have been developed. It provides a virtual experiment for user to predict the situation of an object after it undergoes the given conditions. In product development process, engineer used the FEA to optimize the product and improve the product by predict the weak point, area of tension etc. The result of the simulation will be shown by a color scale where the red color indicates the weaker point or biggest stress of the design. In order to simulate an object in given condition, a mesh is needed to create before starting the simulation. It divides the structure into a million of small elements. The purpose of meshing process is to distribute the load uniformly to the structure. After that, the calculation is done for each single element and the result of the simulation that obtain from the combination of each individual calculation will be shown by color scale (Jayasudha *et al.*, 2015).

2.6.2 Advantages of FEA

The main advantage of FEA is that it provides a virtual testing place for engineer to test the design without the prototype. Engineer can use the FEA to improve the design quality and made the product more competitive compare to traditional technique. Thus, it has been replacing the traditional technique across many industries. In traditional product development process, it usually involves the process of retest and redesign after the prototype has been manufactured. Those process actually waste a lot of time, material and cost. By using FEA, engineer can redesign their product within a shorter time in the FEA software when the weaker point of the structure has been discovered. Moreover, the accuracy of FEA is higher than the traditional product development process. This is because the FEA can predict the situation at each point of structure (*Virtual Prototyping and How It Can Benefit Your Product Design Process*, n.d.). Figure 2.8 shows the difference between the traditional technique and FEA.

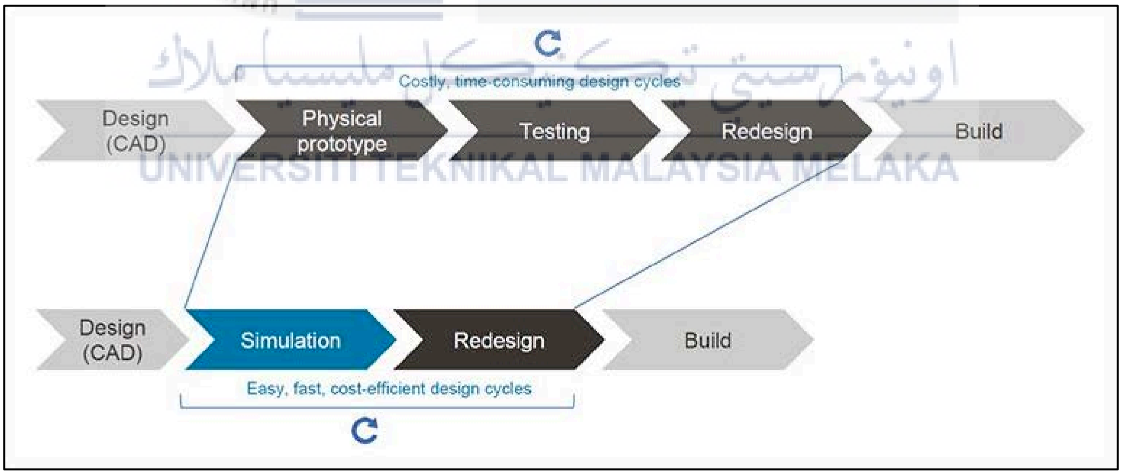

Figure 2.8: Difference between the traditional technique and FEA

(Sources: simscale.com)

2.6.3 Limitation of FEA

FEA is a high level of technology. In product development process, it helps the engineer to accelerate the process of design become faster and efficient. However, the result obtain from the FEA is based on the input parameter that enter by engineer. Once the engineer enters the wrong information, the result obtain from FEA may be not accurate anymore. Thus, the result obtains from FEA need to compare with the hand calculation or prototype testing result.

2.6.4 Application of FEA

FEA has a various application across the different industries. Due to the characteristics of saving time and money in product development process, FEA become a favorite technique in many companies. It can be used in the various field such as mechanical engineering, geotechnical engineering, aerospace engineering, nuclear engineering, electrical and electronic engineering, metallurgical, chemical engineering, meteorology and bio-engineering. In mechanical engineering, FEA can use to understand the structure from steady and transient thermal analysis, stress analysis, design and analysis, and manufacturing process. In this research, FEA is used to complete the steady and transient thermal analysis for different design of disc brake rotor.

2.6.5 FEA Software (ANSYS)

ANSYS is a simulation software that developed by Dr. John A. Swanson in 1970. It was developed to solve the structure problem. The application that can be solve by ANSYS included structure, thermal, electrical, fluid problem, and biological component. During the product development process, thermal management is an important factor, heat energy that released or absorbed by structure need to be consider. Simulation using ANSYS before production can improve the lifetime of the product as well as safety feature because a high temperature can cause destruction to the product and lead to dangerous case. Furthermore, simulation can eliminate the waste of money, material, and time. By using the ANSYS to simulate the design, suitable material can be selected to reduce the cost and maximize the lifetime (ANSYS Advantage, 2009). This is because the respond of material under the condition can be predicted before manufacture the product. There are three type of ANSYS software routinely used by today engineer, which is ANSYS Mechanical, ANSYS Fluent, and ANSYS Icepak.

2.6.6 Steady State Thermal Analysis

Steady state thermal analysis is a type of analysis that calculate the effects of steady thermal loads on a component or system. Steady thermal loads mean that the temperature distribution and thermal flows in a system or component is remain constant from time to time. It usually performs before the transient thermal analysis. This is because the initial condition that needed in transient thermal analysis can be establish using steady state thermal analysis. It can used to analyze the temperature, thermal gradient, heat flow rates and heat flux that under the thermal load such as convection, radiation, heat flow rate, heat flux, heat generation rate, and constant temperature boundary.

2.6.7 Transient Thermal Analysis

Transient thermal analysis is a type of analysis that determines temperature and other thermal quantities that vary over time. A transient thermal analysis has a same procedure as steady state thermal analysis, but the main difference is that the applied load in transient thermal analysis are the function of time. The initial condition needs to define and time stepping solutions needs to carry out for the thermal load of the boundary condition. The transient thermal analysis can use to determine temperature in the application such as heat treatment problem, nozzle, engine block, piping system, pressure vessel, etc.

2.7 Review of Previous Research

Shahril *et. al* (2014) present a paper on Thermal Effects of Disc Brake Rotor Design for Automotive Brake Application. The objective of its paper is to identify the temperature distribution and heat transfer rate on solid disc, ventilated disc, and drilled disc. In this case, the result of three types of design is compared. The drilled disc can dissipate a large amount of heat compare to solid disc and ventilated disc. This is because the drilled geometry increases the rate of air flow around the disc (Shahril *et. al*, 2014). Therefore, the drilled disc shows a lower surface temperature compare to ventilated disc and solid disc.

Amrish (2016) perform an analysis on different design of disc brake rotor. The purpose of this research is to investigate the different type of disc brake rotor that commonly use in the vehicle, which is solid rotor and drilled rotor. A structure analysis and steady state thermal analysis is done for each design. The result shows that the stress, strain, overall deformation and thermal stability of drilled rotor is better than the solid rotor. Hence the drilled rotor is usually used in performance car such as sport car. However, the drilled rotor is difficult to manufacture and hence, automotive industry usually prefers solid rotor.

Priyadarsini (2017) present a paper to study the effect of slotted holes on performance of disc brake. The objective of this paper is to analyze the thermo mechanical behavior of the dry contact of the brake disc during the braking phase. Cast iron and stainless steel is used to analyze the temperature and deformation of slotted disc brake rotor. The coupled thermal-structural analysis is used to analyze the thermal stresses and calculate the heat fluxes in *x-y-z* planes. The slotted disc of cast iron shows a lower temperature and deformation compared to stainless steel. For the cast iron, there is a reduction about 33 % in temperature and 75 % in deformation compared to stainless steel.

Hingu (2017) perform a thermal analysis on disc brake rotor. The main purpose of his paper is to identify the function of the hole on disc brake rotor. A transient thermal analysis is used to determine the temperature distribution of two type of disc brake rotor at different time interval. Both of the simple rotor and perforated rotor has a same material and dimension. A high temperature of 400 °C is used to attain on the simple rotor and perforated rotor. The result shows that the perforated rotor has a lower maximum temperature compared to the simple rotor after fifty seconds.

According to the Deshpande and Kamat (2017), a proper heat dissipation is required to avoid the disc failure. The objective of this paper is to study the issues of brake failure due to overheating and the method to reduce failure. During the suddenly hard braking condition, the temperature on the surface of rotor can reach to a high temperature of 900℃ in a fraction of second. In this condition, a larger amount of plastic deformation and thermal stress will be generated on the surface of rotor and lead to the thermal cracking of rotor. Therefore, a proper material and ventilation is needed to increase the rate of convection.

CHAPTER 3

METHODOLOGY

3.1 Introduction

The main purpose of this chapter is to describe the method to achieve the objective of the project. Steady state thermal analysis and transient thermal analysis is used to analyze the temperature and deformation of the disc brake rotor. Static structure analysis and transient structure analysis is used to determine the deformation and stress of the disc brake rotor. In this project, four ventilated disc brake rotors with different design specification is compared. The detail dimension of disc brake rotor is collected and recorded. The 3D model of four different design specification of ventilated disc brake rotor is drawn in SolidWorks. In order to analyze the temperature and deformation of ventilated disc brake rotor, a process of meshing and simulation is completed by using a FEA software, ANSYS. The final result is compared and discussed.

3.2 Overall Process

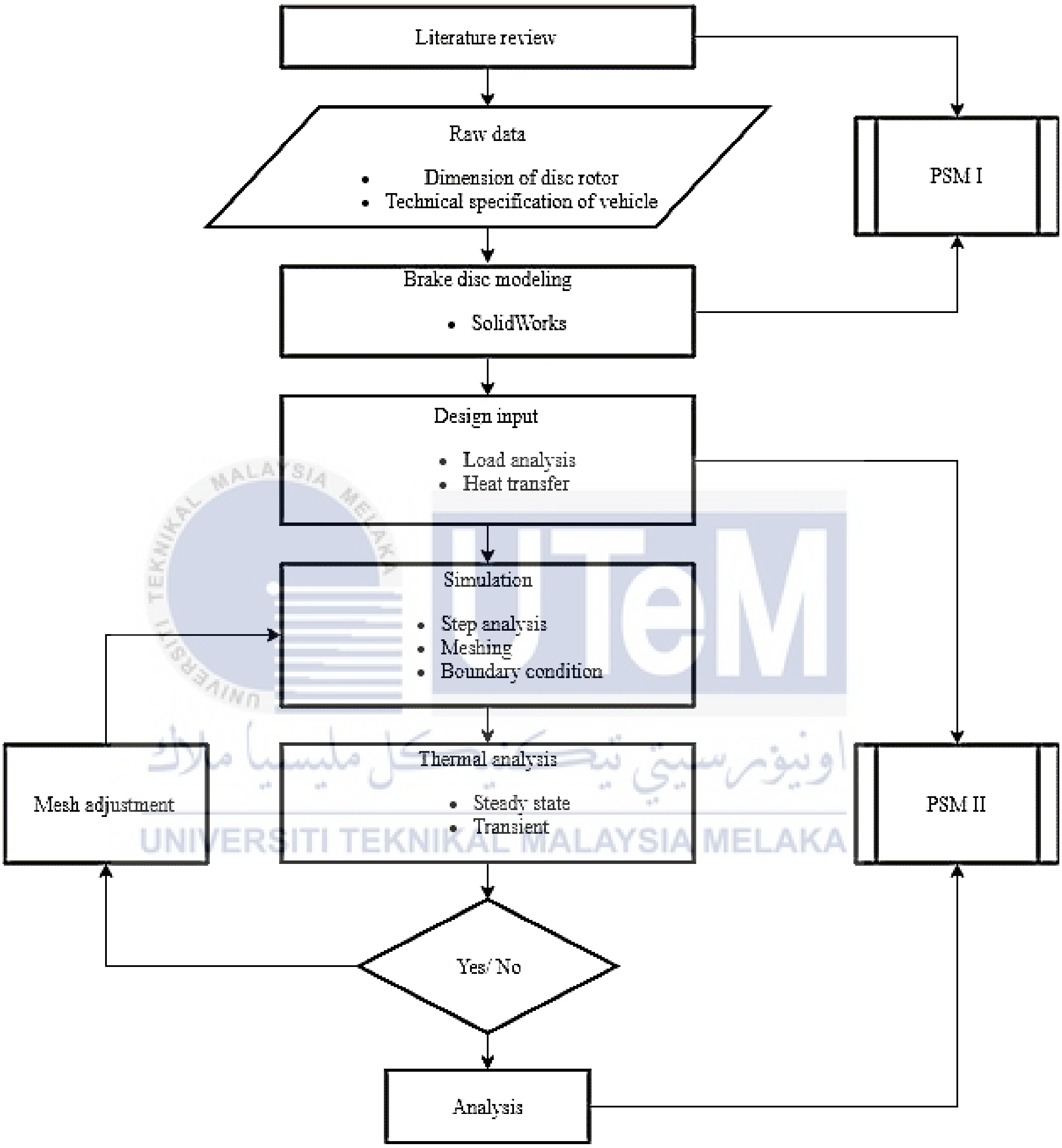

Figure 3.1: Flow chart of overall process

Figure 3.1 shows the flow chart of this project, the overall process that needed to achieve the objective is described in this flow chart. This project starts with the literature review and end with the result of FEA. Literature review involve the detail theory that relating to the disc brake rotor. The related theory such as working principle, trend of industry, heat transfer, and finite element analysis is explained in the literature review. The data such as technical specification of vehicle and dimension of disc brake rotor is collected and recorded. SolidWorks is used to design the model of disk brake rotor.

The calculation for the heat transfer on the disc brake rotor is completed before the process of simulation. All of the four different design of disc brake rotor that drawn in SolidWorks is analyzed by the FEA software, ANSYS. In this step, the process of meshing, step analysis, and boundary condition is carried out by using the ANSYS. The steady state thermal analysis and transient thermal analysis is used to analyze the four discs brake rotor. If the result of the simulation is not accurate, a repeating process is needed to analyze the disc brake rotor.

3.3 Raw Data Correction

3.3.1 Technical Specification of Vehicle

Honda Civic is a high-performance vehicle that used by Malaysian. This is a tenth generation of Honda Civic. A high-performance can be defined as a vehicle that designed and constructed for the requirement of speed. It has a higher horsepower compared to normal vehicle. Honda Civic use the ventilated disc at all the four wheels. This is because a strong braking power is needed for the higher horsepower of vehicle to slow down or stop. Therefore, a large amount of heat will be generated on the disc brake rotor. In this project, a thermal stress analysis on different design of disc brake rotor is done by using the ANSYS software. Figure 3.2 shows the Honda Civic. Table 3.1 shows the technical specification of Honda Civic.

Figure 3 2: Honda civic

(Source: auto123.com)

Table 3.1: Technical specification of Honda Civic

(Sources: www.auto123.com)

No	Specification	Description
1	Curb weight	1247 *kg*
2	Height	1416 *mm*
3	Length	4631 *mm*
4	Width	1878 *mm*
5	Brake type	4 wheels disc
6	Wheelbase	2700 *mm*
7	Tires	P215/55R16 tires
8	Diameter of tires	25.3 *inches* / 642.62 *mm*

The gross weight of car can be calculated by using the Eq. (3.1):

$$\text{Gross weight} = \text{Curb weight} + \text{Load} \tag{3.1}$$

Where;

Curb weight, N = Total weight of vehicle without passenger

Load, N = Weight of passenger and luggage

In order to complete the load analysis, power and weight of vehicle is the important parameter that can affect the braking power. According to the user manual of Honda Civic, the maximum load that can carry by the vehicle is 385 *kg* (Honda, 2018). It means that the combined weight of the luggage and passenger cannot exceed 385 *kg*. In this project, a 385 *kg* of load is used to determine the maximum heat that can be generated on the surface of rotor. The dimension of disc brake rotor for Honda Civic is shows in Table 3.2. It is one of the available disc brake rotor for Honda Civic. Figure 3.3, 3.4, 3.5, and 3.6 shows the isometric view of each rotor.

Table 3.2: Dimension of disc brake rotor for Honda Civic

(Source: www.carid.com)

No	Specification	Description
1	Rotor Height	46.80 *mm*
2	Hub hole diameter	64.00 *mm*
3	Minimum rotor thickness	21.00 *mm*
4	Nominal rotor thickness	22.00 *mm*
5	Outside diameter	282.00 *mm*
6	Rotor material	Cast iron
7	Bolt circle	114.3 *mm*
8	Stud size	12.70 *mm*

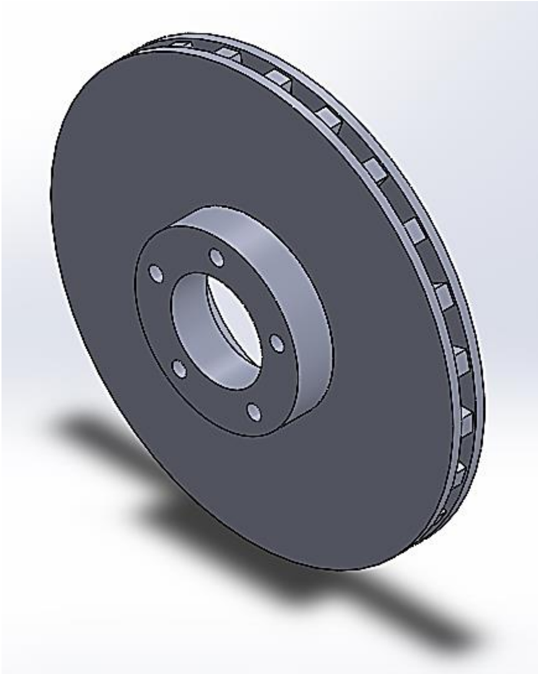

Figure 3.3: Isometric view of blank rotor

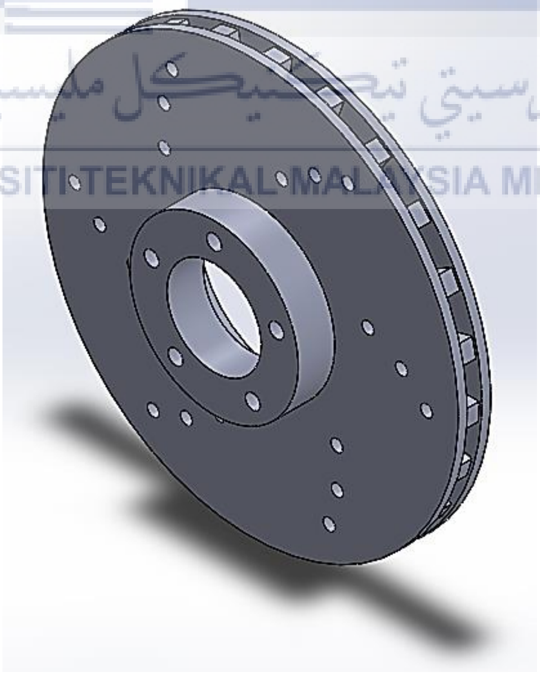

Figure 3.4: Isometric view of drilled rotor

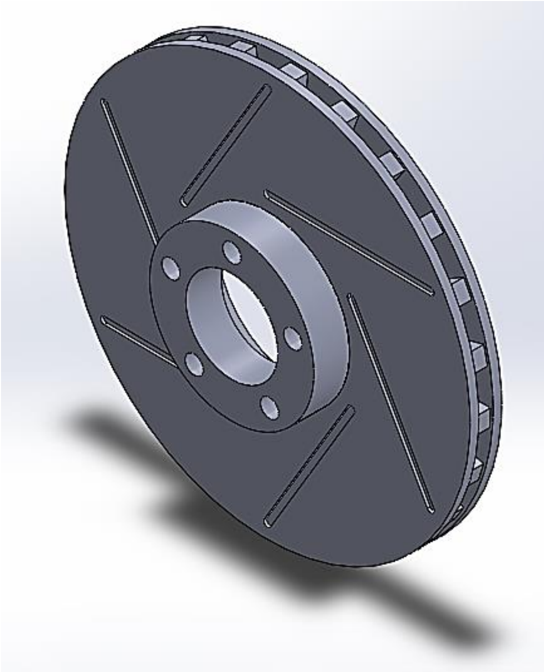

Figure 3.5: Isometric view of slotted rotor

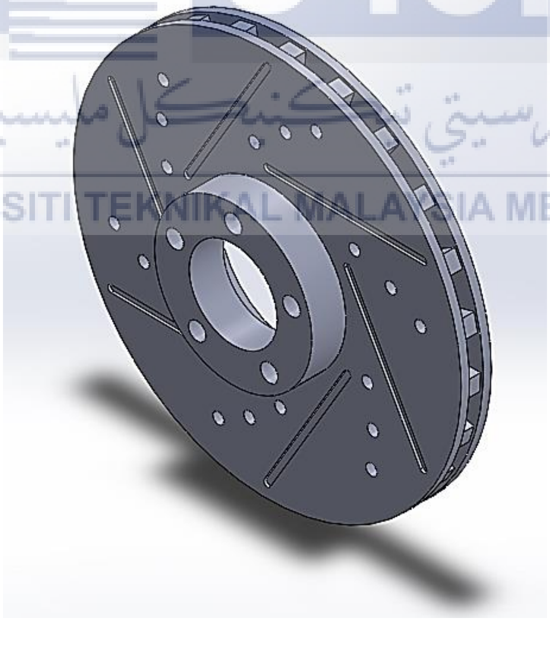

Figure 3.6: Isometric view of slotted and drilled rotor

CHAPTER 4

LOAD ANALYSIS

4.1 Introduction

A tetrahedral method is used to generate the mesh on the rotor. The total heat flux generated on the surface of rotor and convective heat transfer coefficient for certain surface that exposed to the air is calculated and recorded. After that, the reference value of each parameter is inserted into the ANSYS for further analysis. According to Greibe (2007), if the speed of a vehicle is 110 km/h, it required a distance of 159 meters to stop. This information is applied in this analysis. Based on Limpert (2011), 55 % of total kinetic energy is converted into the thermal energy on front disc brake rotor and the heat dissipate by radiation is ignored due to only small amount of heat is dissipated by radiation which is 5 % to 10 %. The heat dissipate by conduction is ignored due to the conduction is speed independent. It means that the amount of heat dissipate by conduction is a constant value. Therefore, only convection is involved in this analysis. The inertia temperature of this rotor is 303 K (Voller 2003). Convective heat transfer coefficient that calculated for each part is labelled in Figure 4.1 by alphabet. Surface A and B is the annular ring surface. Surface C and D is cylindrical surface. Surface E is vane area.

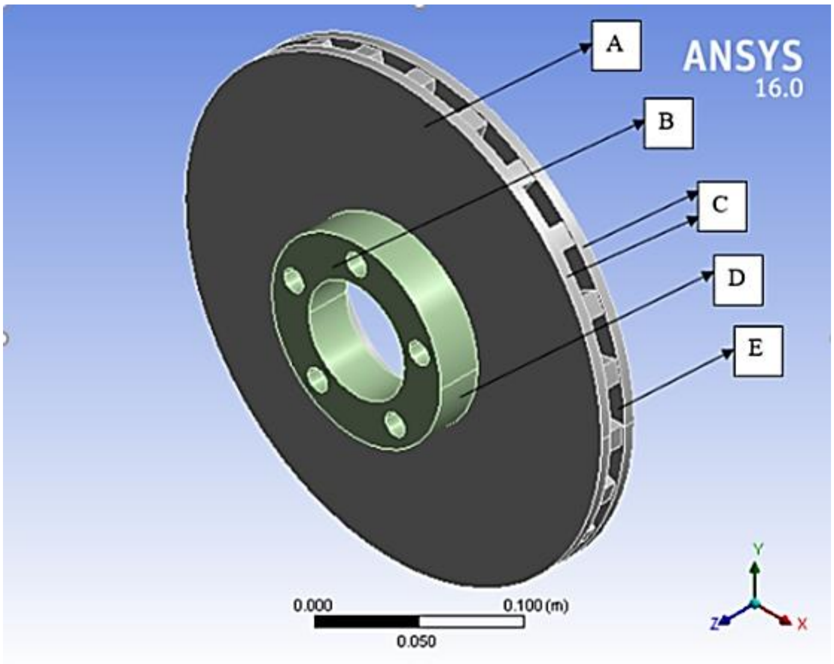

Figure 4.1: Model of blank rotor with alphabet label

4.2 Heat Flux

1 According to Limpert (2011), maximum braking power in a braking condition is at time, $t = 0\ s$ and it is shows in Eq. (4.1).

$$P_b = -kmaV_1 \tag{4.1}$$

2 Based on Limpert (2011), the energy dissipated by the front disc is equal to 55% of total kinetic energy. The Eq. (4.1) is multiply by 0.55.

$$P_b = -kmaV_1(0.55) \tag{4.2}$$

3 Therefore, the total energy dissipated by one of the front disc brake rotor is multiply by 0.5 because there are two rotors located in front of the car. The Eq. (4.2) is multiply by 0.5.

$$P_b = -kmaV_1(0.55)(0.5) \tag{4.3}$$

4 Eq. (4.3) is used to calculate the braking power generated on a front disc brake rotor.

$$P_b = -kmaV_1(0.55)(0.5)$$

Gross weight of vehicle, m $= 1247 + 385 = 1632\ kg$

Time to stop, t $= 5\ s$

Velocity, V $= 110\ km/h = \frac{110\times1000}{60\times60} = \frac{275}{9} = 30.56\ ms^{-1}$

Deceleration, a $= \frac{30.56}{5} = 6.11\ ms^{-2}$

Correction factor of rotating mass, k $= 1$ (constant)

$$P_b = -1(1632)(6.11)(30.56)(0.55)(0.5)$$

$$= 83815.89333\ W$$

5 Based on Manjunath T.V. and Dr Suresh P.M. (2013), heat flux generated on two friction surfaces of rotor:

$$\text{Heat flux} = \frac{P_b}{A} \quad (4.4)$$

Outer radius of rotor, r_0 $= 0.141\ m$

Inner radius of rotor, r_i $= 0.05715\ m$

Area of annual ring surface, A $= 2(\pi {r_0}^2 - \pi {r_i}^2)$

$= 2\,\pi\ (0.141^2 - 0.05715^2)$

$= 0.1044\ m^2$

$$\text{Heat flux} = \frac{83815.89333}{0.1044} = 802834.2273\ Wm^{-2}$$

Therefore, heat flux generated on one surface of rotor is:

$$\text{Heat flux} = \frac{802834.2273}{2} = 401417.1137\ Wm^{-2}$$

4.3 Reynold Number

1 Rotating Reynolds number, Re_o:

$$Re_o = \frac{\omega r^2}{v} \tag{4.5}$$

Radius of tire, r $= 0.32131\ m$

Velocity of vehicle, V $= 110\ km/h = \frac{110\times1000}{60\times60} = \frac{275}{9} = 30.56\ ms^{-1}$

Angular velocity of tire, ω $= \frac{V}{r} = \frac{30.56}{0.32131} = 95.1\ s^{-1}$

Kinematic viscosity of air at 303 K, v $= 1.568\times10^{-5}m^2s^{-1}$

Radius of rotor, r $= 0.141\ m$

$$Re_o = \frac{95.1\times0.141^2}{1.568\times10^{-5}} = 1.2058\times10^5$$

2 Cross flow Reynolds number, Re_t:

$$Re_t = \frac{V\mathrm{r}}{v} \tag{4.6}$$

Velocity of vehicle, V $= 110\ km/h = \frac{110\times1000}{60\times60} = \frac{275}{9} = 30.56\ ms^{-1}$

Radius of rotor, r $= 0.141\ m$

Kinematic viscosity of air at 303 K, v $= 1.568\times10^{-5}m^2s^{-1}$

$$Re_t = \frac{30.56\times0.141}{1.568\times10^{-5}} = 2.75\times10^5$$

4.4 Convective Heat Transfer Coefficient for Annular Ring Surface

According to (Limpert, 2011), if the rotating Reynold number of a rotating surface is smaller than 240 000, it is a laminar flow. The Eq. (4.7) from (Tsai *et. al*, 2007) is used to calculate convective heat transfer coefficient on the annular ring surface. Voller (2003) states that the value of thermal conductivity of air at 303 *K* is $2.624 \times 10^{-2}\ Wm^{-1}K^{-1}$.

$$h_{conv} = 3.974 \times \frac{k_a}{d} \times {Re_o}^{0.55} \tag{4.7}$$

Thermal conductivity of air at 303 *K*, k_a $= 2.624 \times 10^{-2} Wm^{-1}K^{-1}$

Outer diameter of rotor, D $= 0.282\ m$

Rotating Reynolds number, Re_o $= 1.2058 \times 10^5$

h_{conv} for annular ring surface A with outer diameter of 0.282 *m*:

$$h_{conv} = 3.974 \times \frac{2.624 \times 10^{-2}}{0.282} \times (1.2058 \times 10^5)^{0.55}$$

$$= 230.5\ Wm^{-2}K^{-1}$$

h_{conv} for annular ring surface B with outer diameter of 0.1143 *m*:

$$h_{conv} = 3.974 \times \frac{2.624 \times 10^{-2}}{0.1143} \times (1.2058 \times 10^5)^{0.55}$$

$$= 568.6524\ Wm^{-2}K^{-1}$$

4.5 Convective Heat Transfer Coefficient for Cylindrical Surface

According to (Tsai *et al.*, 2007), Eq. (4.8) is used to calculate convective heat transfer coefficient for a cylindrical surface. Voller (2003) states that the value of thermal conductivity of air at 303 K is $2.624 \times 10^{-2}\ Wm^{-1}K^{-1}$, kinematic viscosity of air at 303 K, v is $1.568 \times 10^{-5}\ m^2s^{-1}$, dynamic viscosity of air at 303 K, μ is $1.86 \times 10^{-5}\ kgm^{-1}s^{-1}$, and specific heat at constant pressure of air at 303 K, Cp is $1005.5\ Jkg^{-1}K^{-1}$.

$$h_{conv} = 1.15 \times \frac{k_a}{D} \times \left(\frac{DV}{v}\right)^{0.5} \times \left(\frac{\mu C_p}{k_a}\right)^{\frac{1}{3}} \qquad (4.8)$$

Thermal conductivity of air at 303 K, k_a $= 2.624 \times 10^{-2}\ Wm^{-1}K^{-1}$

Diameter of cylindrical surface, D $= 0.282\ m$

Velocity of vehicle, V $= 110\ km/h = \frac{110 \times 1000}{60 \times 60} = \frac{275}{9} = 30.56\ ms^{-1}$

Kinematic viscosity of air at 303 K, v $= 1.568 \times 10^{-5}\ m^2s^{-1}$

Dynamic viscosity of air at 303 K, μ $= 1.86 \times 10^{-5}\ kgm^{-1}s^{-1}$

Specific heat at constant pressure of air at 303 K, C_p $= 1005.5\ Jkg^{-1}K^{-1}$

h_{conv} for cylindrical surface C with diameter of 0.282 m:

$$h_{conv} = 1.15 \times \frac{2.624\times10^{-2}}{0.282} \times \left(\frac{0.282\times30.56}{1.568\times10^{-5}}\right)^{0.5} \times \left(\frac{1.86\times10^{-5}\times1005.5}{2.624\times10^{-2}}\right)^{\frac{1}{3}}$$

$$= 70.85757\ Wm^{-2}K^{-1}$$

h_{conv} for cylindrical surface D with diameter of 0.1143 m:

$$h_{conv} = 1.15 \times \frac{2.624\times10^{-2}}{0.1143} \times \left(\frac{0.1143\times30.56}{1.568\times10^{-5}}\right)^{0.5} \times \left(\frac{1.86\times10^{-5}\times1005.5}{2.624\times10^{-2}}\right)^{\frac{1}{3}}$$

$$= 111.298\ Wm^{-2}K^{-1}$$

4.6 Convective Heat Transfer Coefficient for Vane Area

Based on Limpert (2011), for a vane area with cross flow Reynolds number, Re_t bigger than 10 000, it is a turbulent flow. The Eq. (4.9) is used to calculate the convective heat transfer coefficient for the vane area, E.

h_{conv} for vane area:

$$h_{conv} = 0.023 \times [1 + (\frac{d_h}{l})^{0.67}] \times Re_t \times 1^{0.8} \times Pr^{0.33} \times \frac{k_{air}}{d_h} \quad (4.9)$$

Length of cooling vane, l $= 0.08015\ m$

Width of vane at mean rubbing radius of rotor, w $= s = r\theta = 0.09908 \times \frac{5\times\pi}{180}$

$= 0.00864636\ m$

Characteristic length at mean rubbing radius of rotor, d_h $= 4w = 0.0346$ m

Specific heat at constant pressure of air at 303 K, C_p $= 1005.5\ Jkg^{-1}K^{-1}$

Cross flow Reynolds number, Re_t $= 2.75 \times 10^5$

Dynamic viscosity of air at 303 K, μ $= 1.86 \times 10^{-5}\ kgm^{-1}s^{-1}$

Thermal conductivity of air at 303 K, k_a $= 2.624 \times 10^{-2}\ Wm^{-1}K^{-1}$

Prandtl number, Pr $= \frac{\mu C_P}{k_{air}} = \frac{1.86\times10^{-5}\times1005.5}{2.624\times10^{-2}}$

$= 0.71274$

$$h_{conv} = 0.023 \times [1 + \left(\frac{0.0346}{0.08015}\right)^{0.67}] \times 2.75 \times 10^5 \times 1^{0.8} \times 0.71274^{0.33} \times \frac{2.624\times10^{-2}}{0.0346}$$

$$= 550\ Wm^{-2}K^{-1}$$

4.7 Convective Heat Transfer Coefficient for Drilled Hole

Eq. (4.10) is used to calculate the convective heat transfer coefficient of a hole that located at the surface of drilled disc brake rotor. Constant heat flux is applied to the hole for this formula. Therefore, Nusselt Number is constant and equal to 4.36.

$$Nu = \frac{hD}{k_a} \tag{4.10}$$

Nusselt Number, *Nu*	= 4.36
Diameter of hole, *D*	= 0.008 *m*
Thermal conductivity of air at 303 *K*, k_a	$= 2.624 \times 10^{-2}\ Wm^{-1}K^{-1}$

$$4.36 = \frac{h(0.008)}{2.624 \times 10^{-2}}$$

$$h = 14.3008\ Wm^{-2}K^{-1}$$

Since there is a total number of eighteen hole located on the annular ring surface A, the value of convective heat transfer is multiplied by 18.

$$h = 14.3008 \times 18 = 257.4144\ Wm^{-2}K^{-1}$$

4.8 Convective Heat Transfer Coefficient for Slotted Area

Based on Teertstra *et al.* (2014), Eq. (4.11) is used to determine the convective heat transfer coefficient of slotted area.

$$Nu = \frac{Qb}{k_a A(T_s - T_a)} \tag{4.11}$$

Total heat transfer rate, W $= 83815.89333\ W$

Width of slot, w $= 0.005\ m$

Thermal conductivity of air at 303 K, k_a $= 2.624 \times 10^{-2}\ Wm^{-1}K^{-1}$

Area of slot, A $= 0.00104078\ m^2$

Temperature of braking surface, T_{bs} $= 708.12\ K$

Temperature of inlet air, T_{air} $= 303\ K$

$$Nu = \frac{83815.89333 \times 0.005}{2.624 \times 10^{-2} \times 0.00104078 \times (708.12 - 303)}$$

$$Nu = 22629.09$$

$$Nu = \frac{hD}{k_a}$$

Nusselt Number, Nu = 22629.09

Diameter of hole, D = 0.005 m

Thermal conductivity of air at 303 K, k_a $= 2.624 \times 10^{-2}\ Wm^{-1}K^{-1}$

$$h = 118757.4563\ Wm^{-2}K^{-1}$$

Table 4.1 below shows a summary of calculation.

Table 4.1: Summary of calculation

Alphabet label	Parameter	Reference value
A	h_{conv} for annular ring surface of rotating rotor with outer diameter of 0.282 m	$230.50000\ Wm^{-2}K^{-1}$
B	h_{conv} for annular ring surface of rotating rotor with outer diameter of 0.1143 m	$568.65240\ Wm^{-2}K^{-1}$
C	h_{conv} for cylindrical surface with outer diameter of 0.282 m	$70.85757\ Wm^{-2}K^{-1}$
D	h_{conv} for cylindrical surface with outer diameter of 0.1143 m	$111.29800\ Wm^{-2}K^{-1}$
E	h_{conv} for vane area	$550.00000\ Wm^{-2}K^{-1}$
F	h_{conv} for drilled hole	$257.41440\ Wm^{-2}K^{-1}$
G	h_{conv} for slotted area	$118757.45630\ Wm^{-2}K^{-1}$
	Braking power generated on a front disc brake rotor	$83815.89333\ W$
	Heat flux generated on two friction surfaces of rotor	$401417.11370\ Wm^{-2}$
	Rotating Reynolds number, Re_o	1.20580×10^5
	Cross flow Reynolds number, Re_t	2.75000×10^5

4.9 Analysis Setup

4.9.1 Steady State Thermal Analysis

In steady state thermal analysis, a constant heat flux of $401417.1137\ Wm^{-2}$ is applied to the annular ring surface A from time $t = 0\ s$ to $t = 350\ s$. The convective heat transfer coefficient for each surface is applied from $t = 0\ s$ to $t = 350\ s$. The initial temperature of each rotor is 303 *K*. Figure 4.2 below shows the setup of steady state thermal analysis.

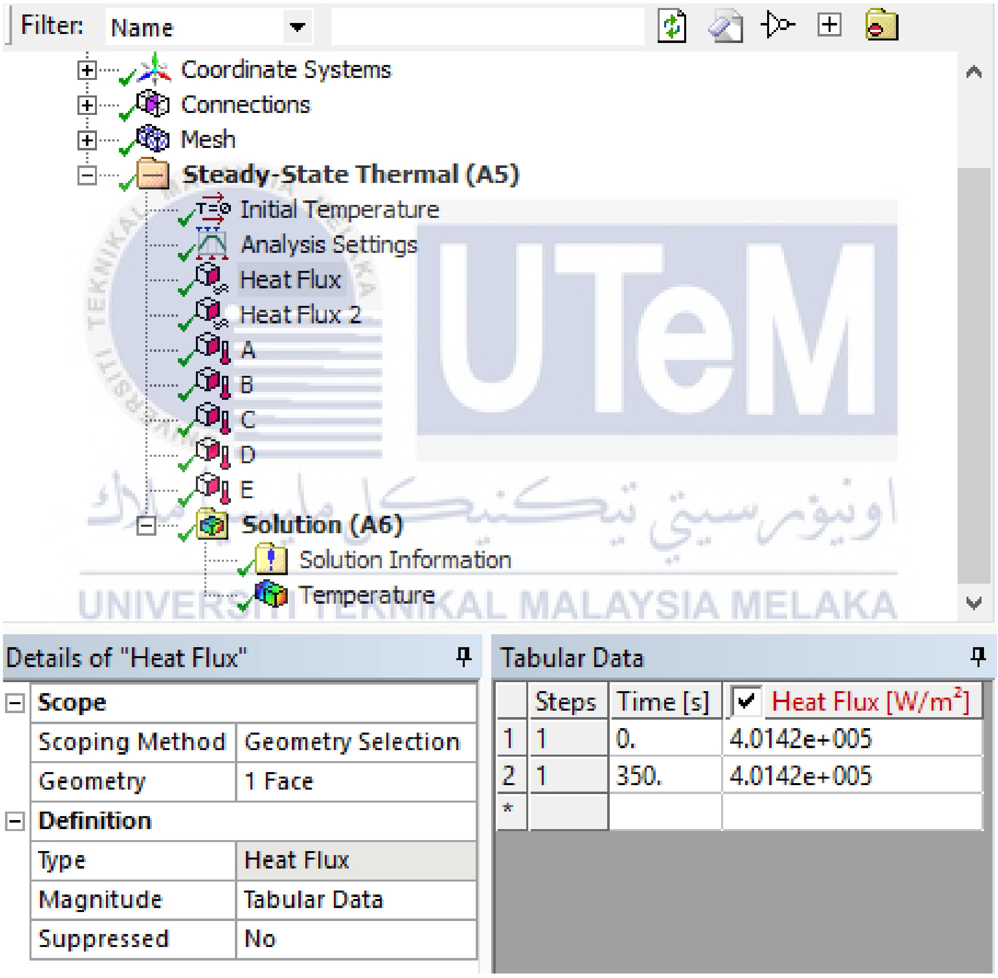

Figure 4.2: Setup of steady state thermal analysis

A material of gray cast iron is selected for the four different design specification of disc brake rotor. Figure 4.3 below shows the material of disc brake rotor.

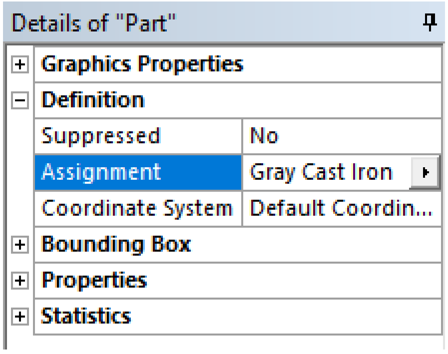

Figure 4.3: Material of disc brake rotor

A tetrahedrons method is used to generate the mesh on rotor. This is because this method can generate a mesh quickly for a complicated geometry. Furthermore, an arbitrary volume can always be filled with tetrahedra. Figure 4.4 below shows the meshing method for all design specification of disc brake rotor.

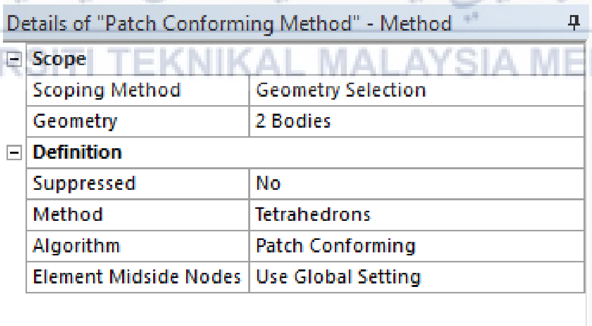

Figure 4.4: Meshing method of all design specification of disc brake rotor

4.9.2 Transient Thermal Analysis

According to Huang and Chen (2006), for transient thermal analysis, 10 load cycle with total time 350 seconds are applied to determine the temperature of disc brake. The heat flux is applied for 6 seconds in each cycle. There will be no heat flux applied to the disc brake for remaining 29 seconds. Therefore, 1 cycle is 35 seconds. This information is applied in transient thermal analysis for 4 discs brake rotor. Voller (2003) stated that the inertia temperature of each rotor is 303 *K*. Figure 4.5 below shows the graph of heat flux versus time.

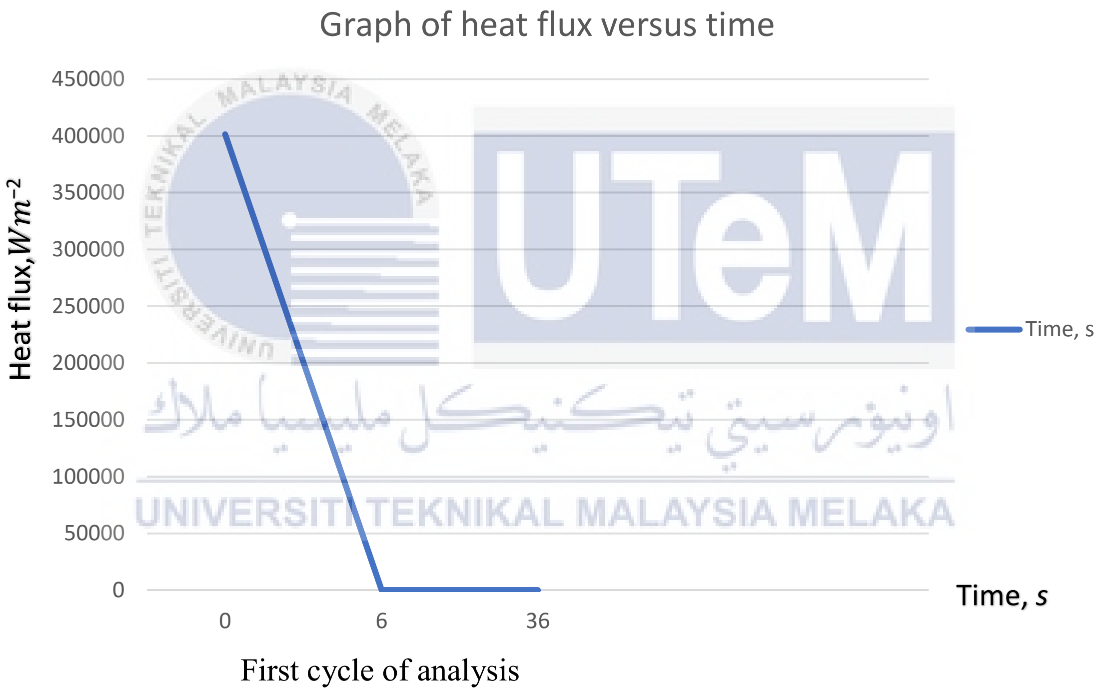

Figure 4.5: Graph of heat flux versus time

4.9.3 Static Structure Analysis

The solution of steady state thermal analysis is used to determine the deformation and equivalent (Von-Mises) stress in static structure analysis. The engineering data and geometry of steady state thermal analysis is transferred to static structure analysis. Figure 4.6 shows the setting of static structure analysis.

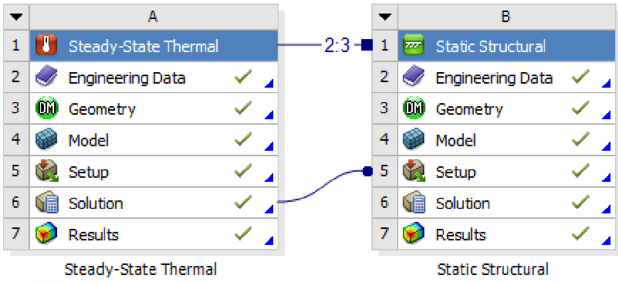

Figure 4.6: Setting of static structure analysis

4.9.4 Transient Structure Analysis

In this transient structure analysis, the engineering data, geometry, and solution of transient thermal analysis is used to determine the deformation and equivalent (Von-Mises) stress of each rotor after several braking operation. Figure 4.7 shows the setting of transient structure analysis.

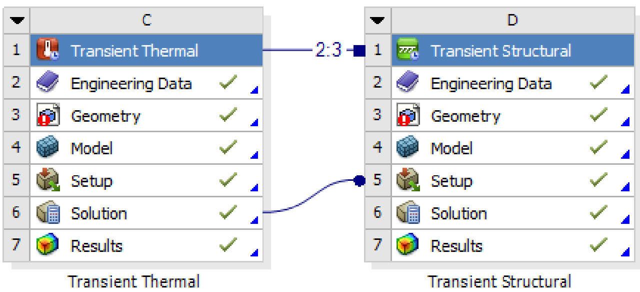

Figure 4.7: Setting of transient structure analysis.

CHAPTER 5

RESULTS AND DISCUSSION

5.1 Results

5.1.1 Steady State Thermal Analysis

For the blank rotor, the maximum and minimum temperature is 981.12 *K* and 480.17 *K*. Figure 5.1 below shows the result of steady state thermal analysis for blank rotor.

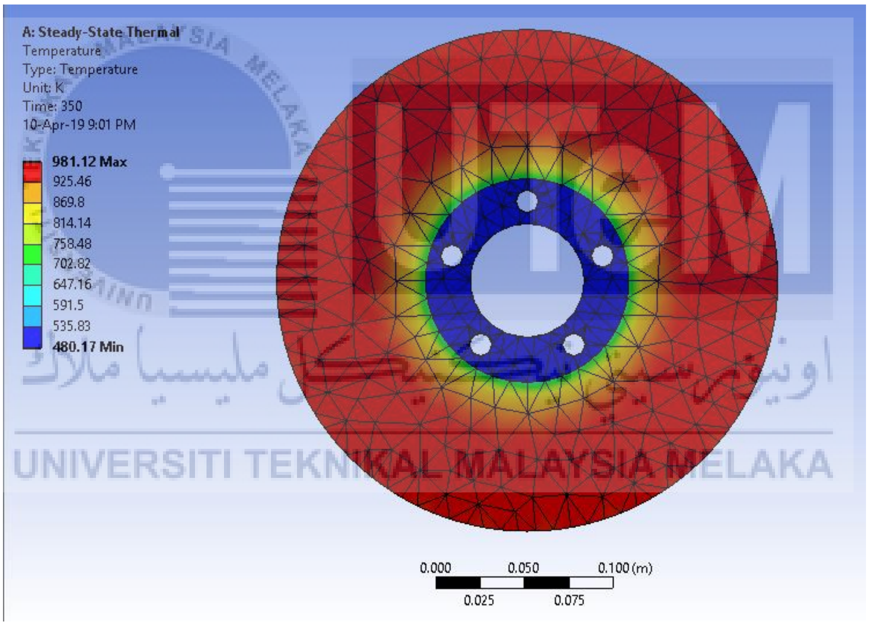

Figure 5.1: Result of steady state thermal analysis for blank rotor

For the drilled rotor, the maximum and minimum temperature is 969.32 *K* and 470.78 *K*. Figure 5.2 below shows the result of steady thermal analysis for drilled rotor.

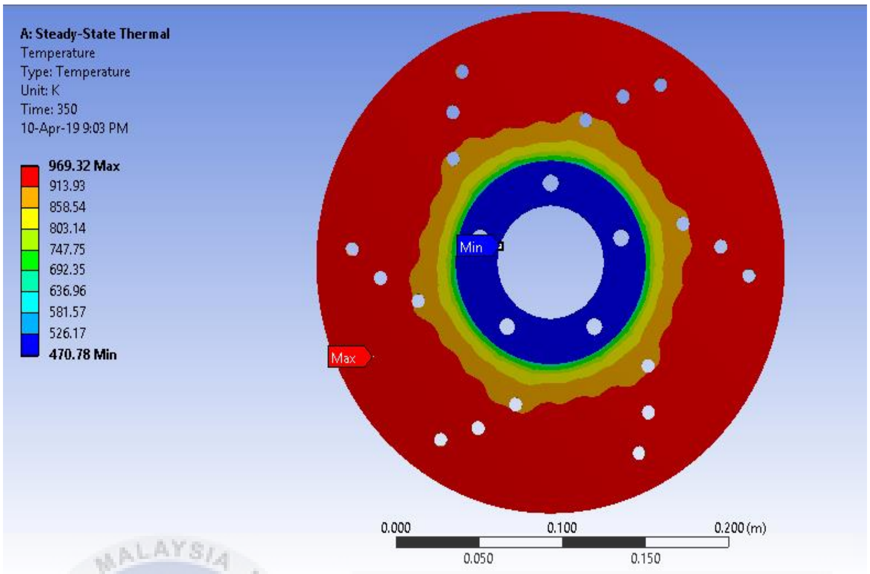

Figure 5.2: Result of steady state thermal analysis for drilled rotor

For the slotted rotor, the maximum and minimum temperature is 803.27 *K* and 303 *K*. Figure 5.3 below shows the result of steady thermal analysis for slotted rotor.

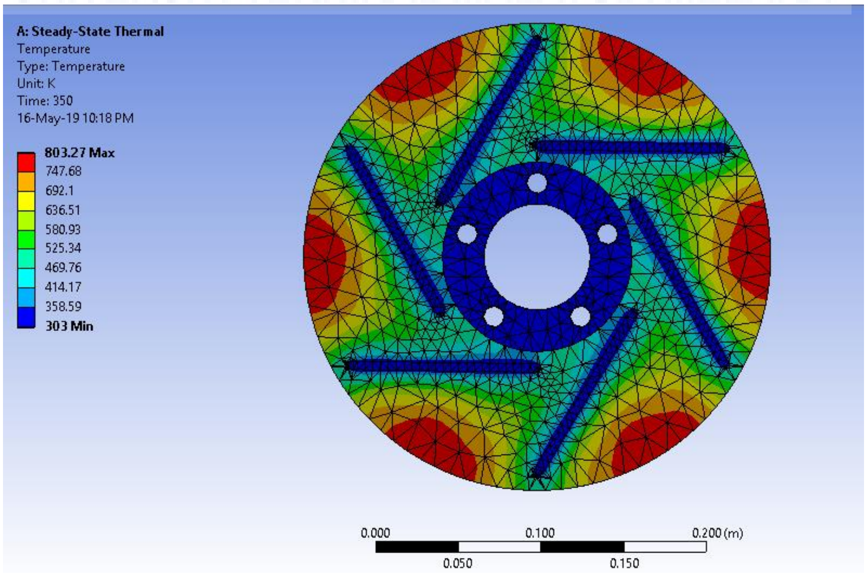

Figure 5.3: Result of steady state thermal analysis for slotted rotor

For the slotted and drilled rotor, the maximum and minimum temperature is 801.86 *K* and 302.03 *K*. Figure 5.4 below shows the result of steady thermal analysis for slotted and drilled rotor.

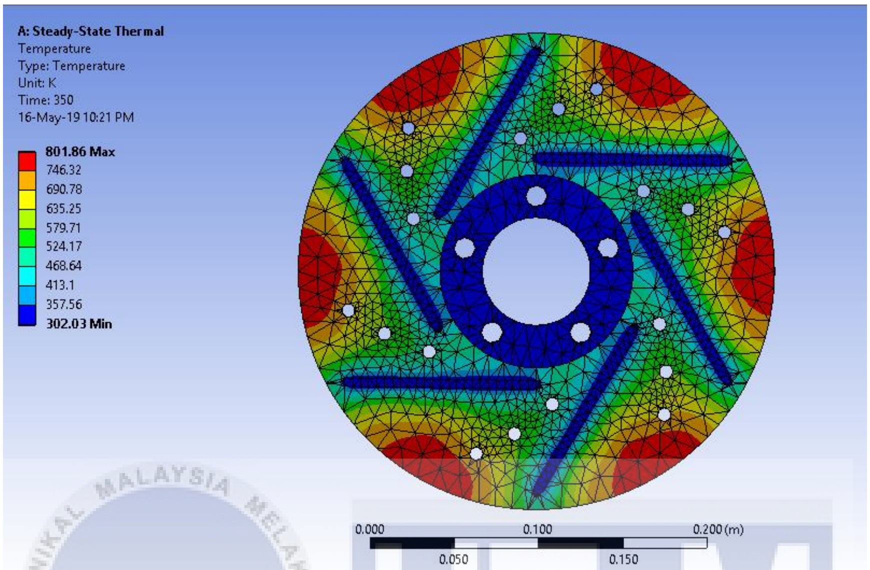

Figure 5.4: Result of steady state thermal analysis for slotted and drilled rotor

5.1.2 Transient Thermal Analysis

For the blank rotor, the maximum and minimum temperature is 651.57 *K* and 303 *K*. Figure 5.5 below shows the result of transient thermal analysis for blank rotor. Figure 5.6 below shows the graph of temperature versus time for blank rotor.

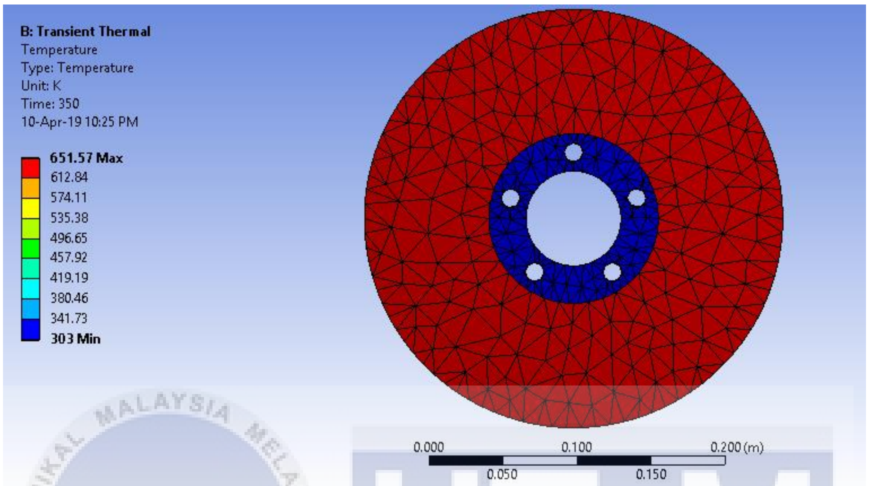

Figure 5.5: Result of transient thermal analysis for blank rotor.

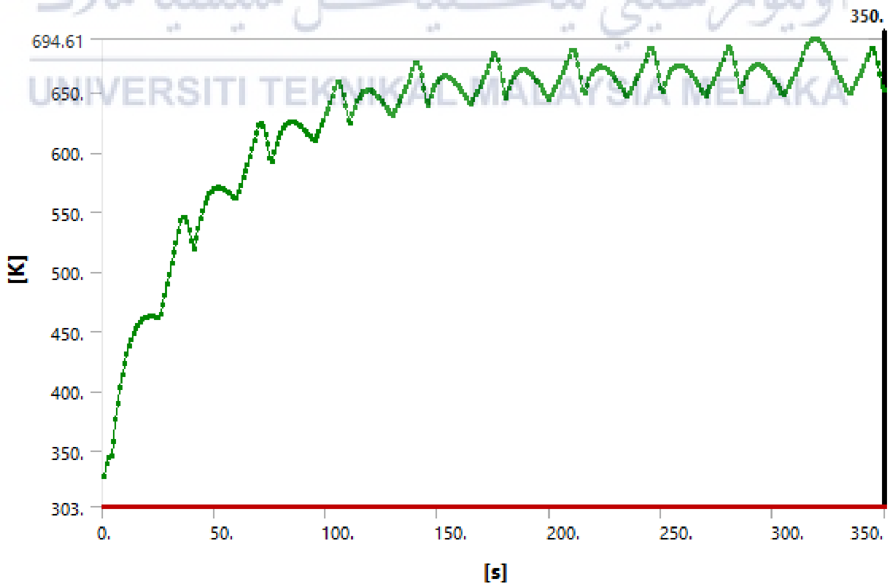

Figure 5.6: Graph of temperature versus time for blank rotor

For the drilled rotor, the maximum and minimum temperature is 635.8 *K* and 303 *K*. Figure 5.7 below shows the result of transient thermal analysis for drilled rotor. Figure 5.8 below shows the graph of temperature versus time for drilled rotor.

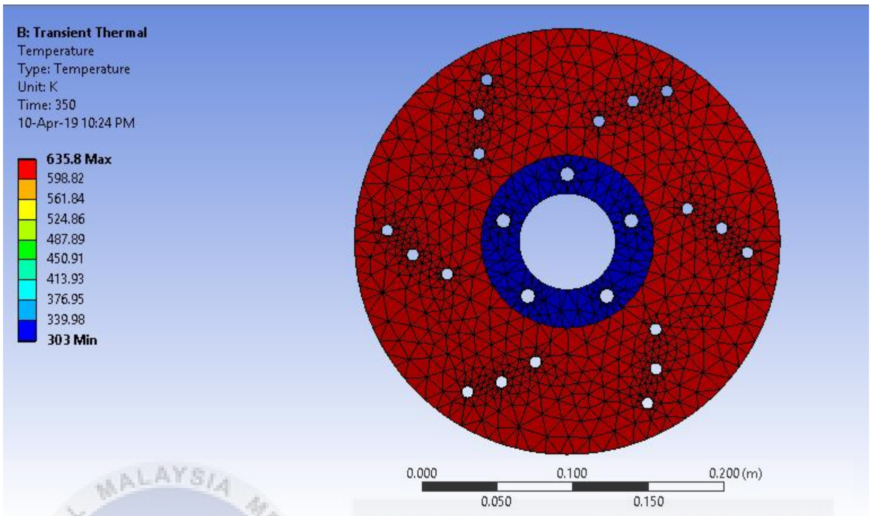

Figure 5.7: Result of transient thermal analysis for drilled rotor

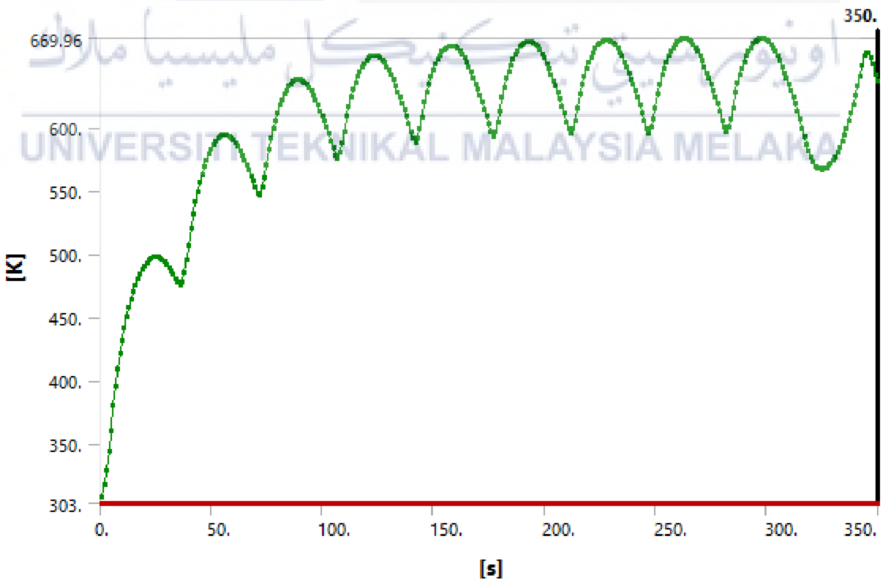

Figure 5.8: Graph of temperature versus time for drilled rotor

For the slotted rotor, the maximum and minimum temperature is 552.68 *K* and 303 *K*. Figure 5.9 below shows the result of transient thermal analysis for slotted rotor. Figure 5.10 below shows the graph of temperature versus time for slotted rotor.

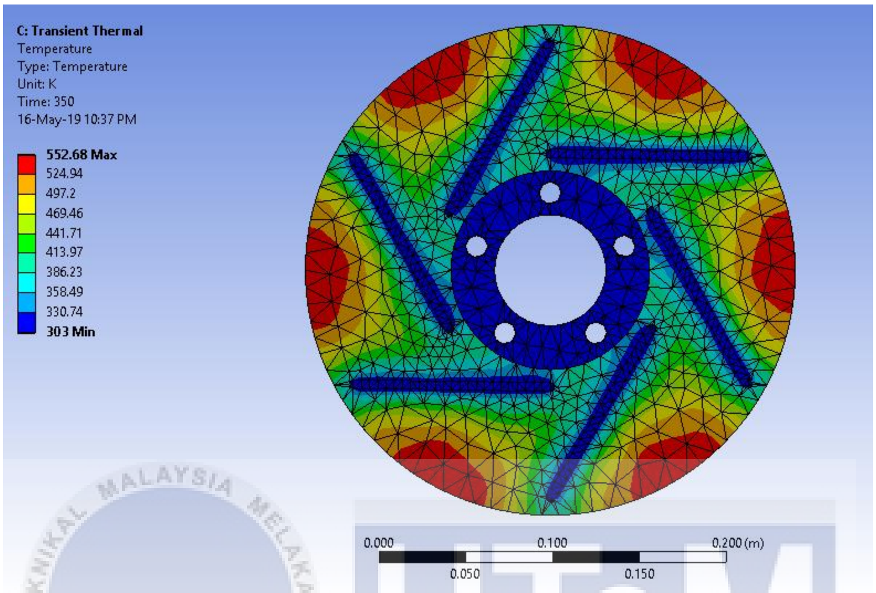

Figure 5.9: Result of transient thermal analysis for slotted rotor

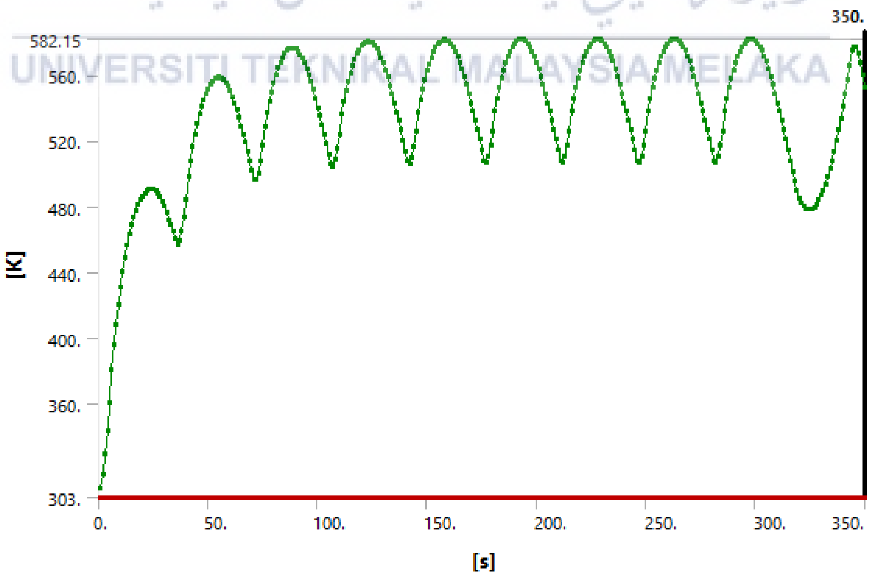

Figure 5.10: Graph of temperature versus time for slotted rotor

For the slotted and drilled rotor, the maximum and minimum temperature is 551.74 *K* and 300.85 *K*. Figure 5.11 below shows the result of transient thermal analysis for slotted and drilled rotor. Figure 5.12 below shows the graph of temperature versus time for slotted and drilled rotor.

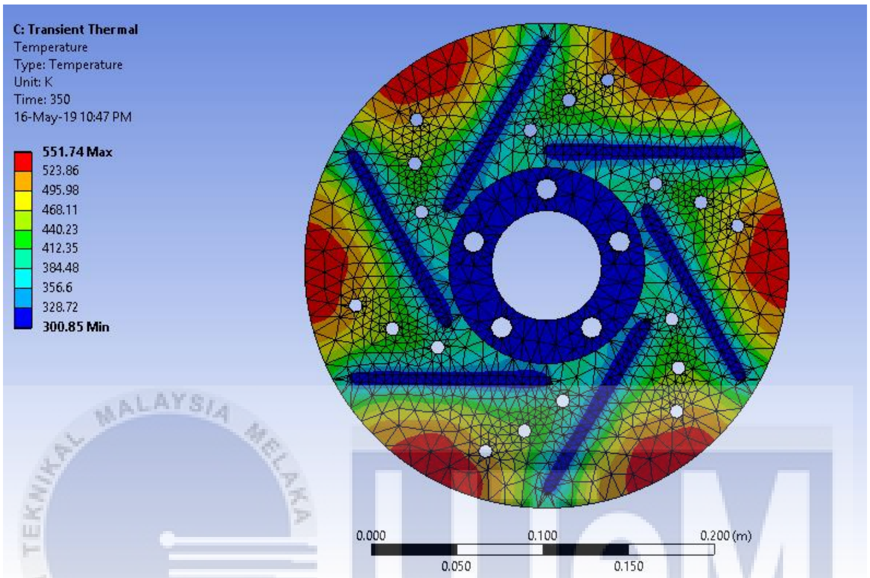

Figure 5.11: Result of transient thermal analysis for slotted and drilled rotor

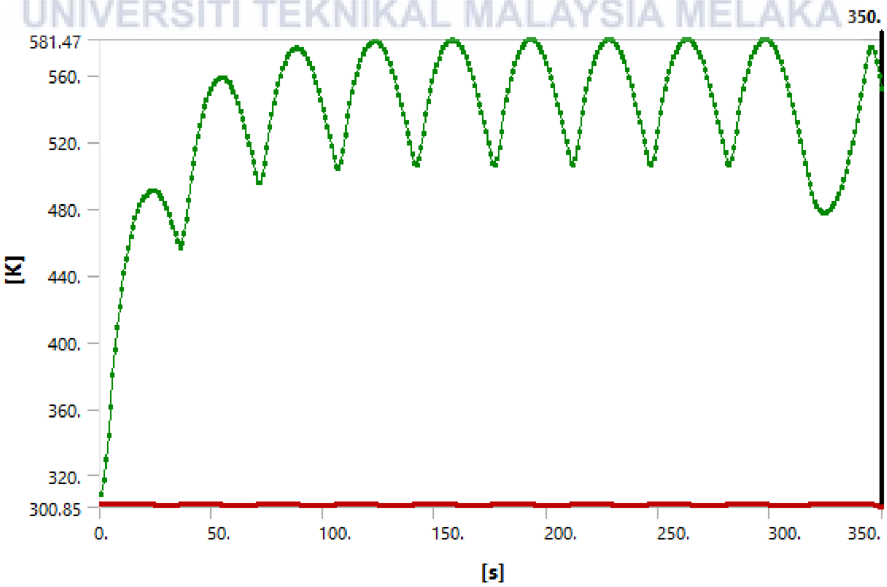

Figure 5.12: Graph of temperature versus time for slotted and drilled rotor

Figure 5.13 below shows the graph of temperature versus time for each type of rotors in transient thermal analysis. The slotted and drilled area increase the rate of heat dissipation and cause the temperature of the rotor become lower.

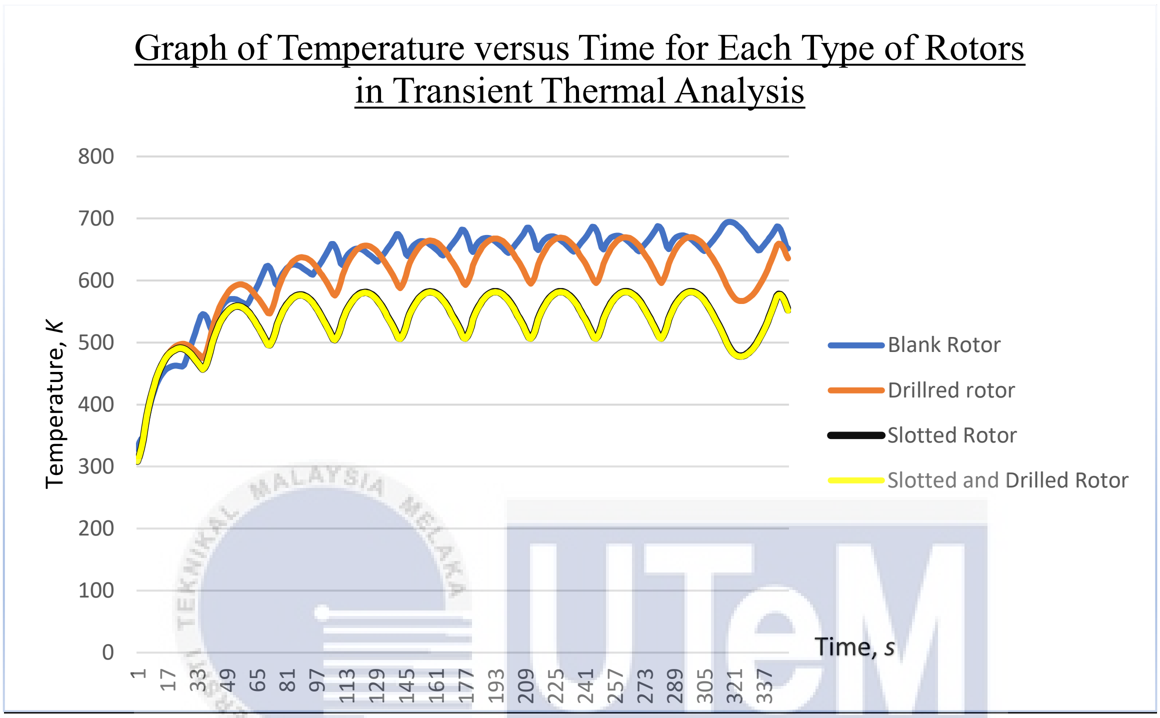

Figure 5.13: Graph of temperature versus time for each type of rotors in transient thermal analysis

5.1.3 Static Structure Analysis

The maximum and minimum deformation of blank rotor in static structure analysis is 0.0010481 m and 0.00019747 m. Figure 5.14 shows the total deformation of blank rotor in static structure analysis.

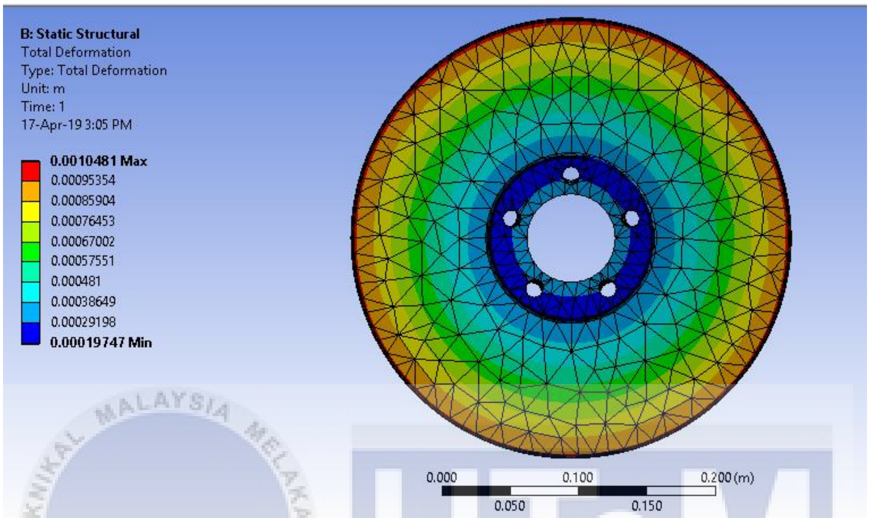

Figure 5.14: Total deformation of blank rotor in static structure analysis

The maximum and minimum equivalent (Von-Mises) stress for blank rotor in static structure analysis is 713.49 MPa and 1.56 MPa. Figure 5.15 shows the equivalent (Von-Mises) stress of blank rotor in static structure analysis.

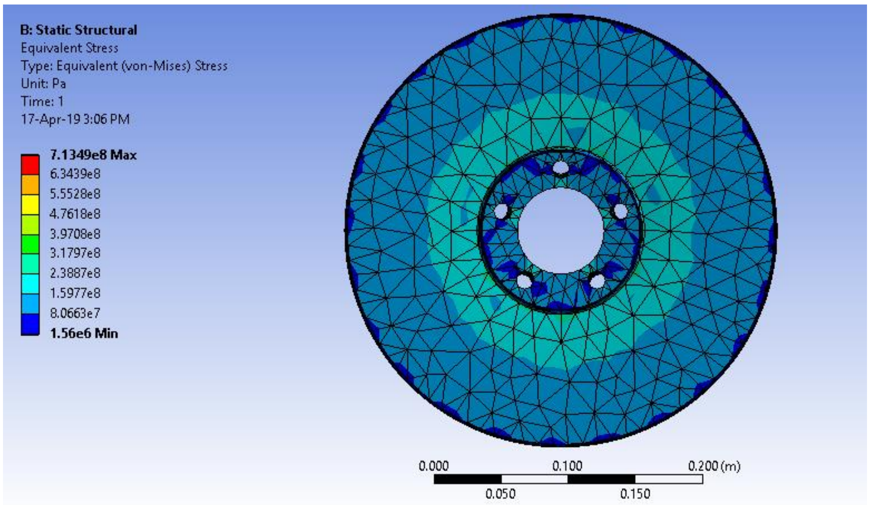

Figure 5.15: Equivalent (Von-Mises) stress of blank rotor in static structure analysis

The maximum and minimum deformation of drilled rotor in static structure analysis is 0.0010144 m and 0.00018567 m. Figure 5.16 shows the total deformation of drilled rotor in static structure analysis.

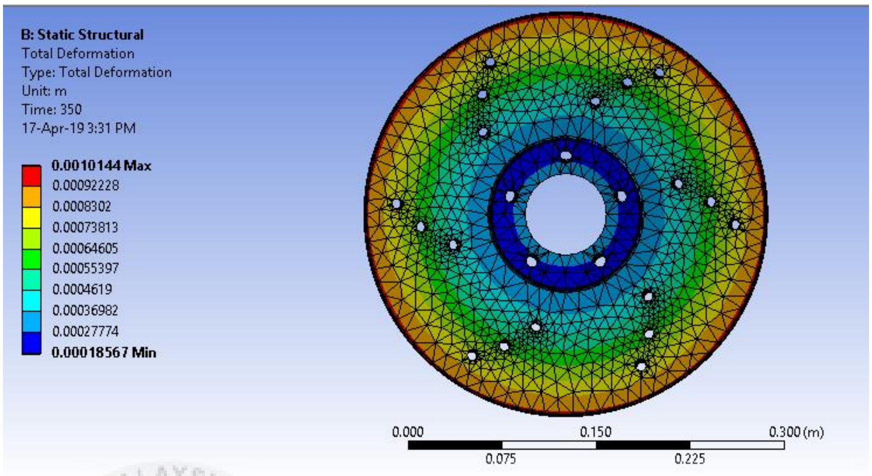

Figure 5.16: Total deformation of drilled rotor in static structure analysis

The maximum and minimum equivalent (Von-Mises) stress for drilled rotor in static structure analysis is 575.66 MPa and 0.74121 MPa. Figure 5.17 shows the equivalent (Von-Mises) stress of drilled rotor in static structure analysis.

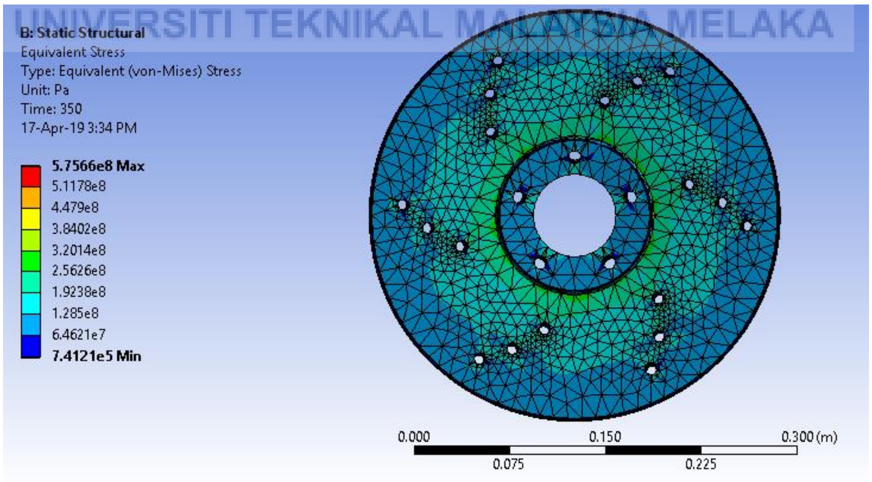

Figure 5.17: Equivalent (Von-Mises) stress of drilled rotor in static structure analysis

The maximum and minimum deformation of slotted rotor in static structure analysis is 0.00046808 m and 0.0000027629 m. Figure 5.18 shows the total deformation of slotted rotor in static structure analysis.

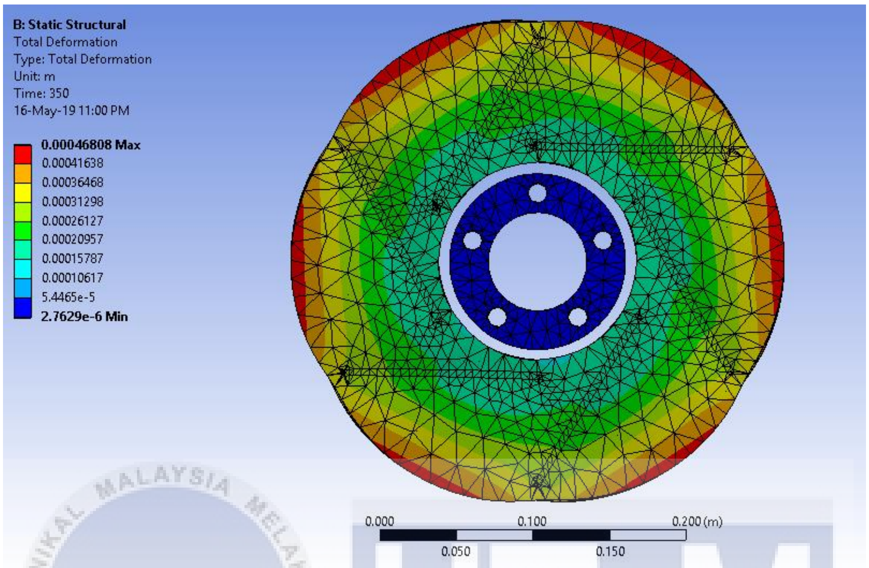

Figure 5.18: Total deformation of slotted rotor in static structure analysis

The maximum and minimum equivalent (Von-Mises) stress for slotted rotor in static structure analysis is 469.23 MPa and 0.00018872 Pa. Figure 5.19 shows the equivalent (Von-Mises) stress of slotted rotor in static structure analysis.

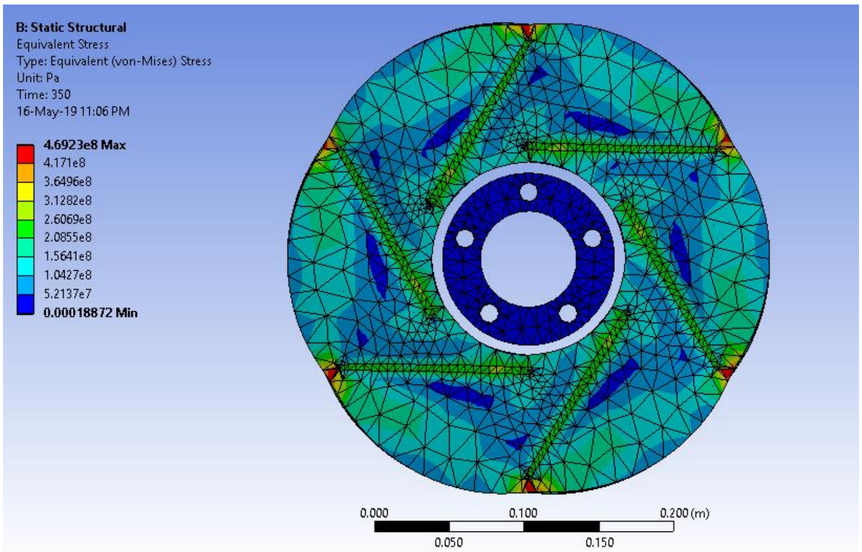

Figure 5.19: Equivalent (Von-Mises) stress of slotted rotor in static structure analysis

The maximum and minimum deformation of slotted and drilled rotor in static structure analysis is 0.00045927 *m* and 0.0000027298 *m*. Figure 5.20 shows the total deformation of slotted and drilled rotor in static structure analysis.

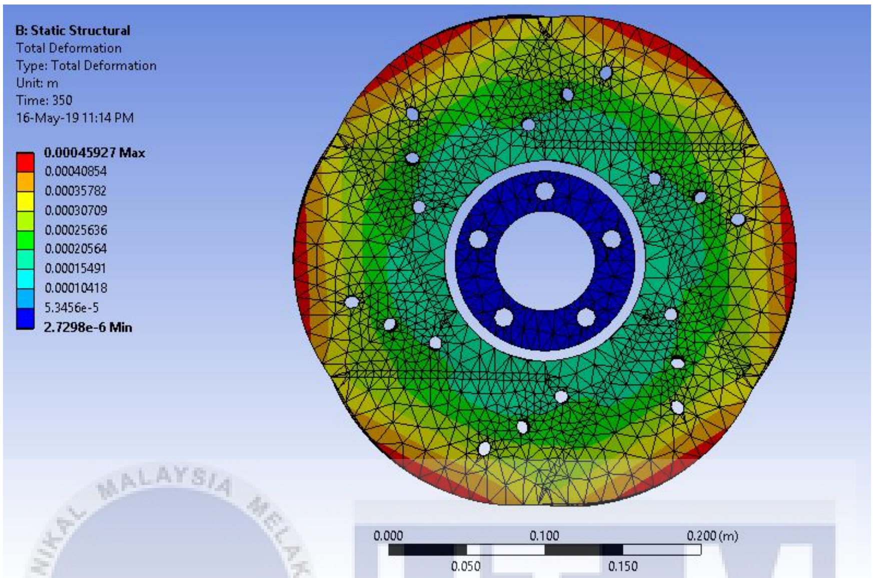

Figure 5.20: Total deformation of slotted and drilled rotor in static structure analysis

The maximum and minimum equivalent (Von-Mises) stress for slotted and drilled rotor in static structure analysis is $825.06\ MPa$ and $0.00022164\ Pa$. Figure 5.21 shows the equivalent (Von-Mises) stress of slotted and drilled rotor in static structure analysis.

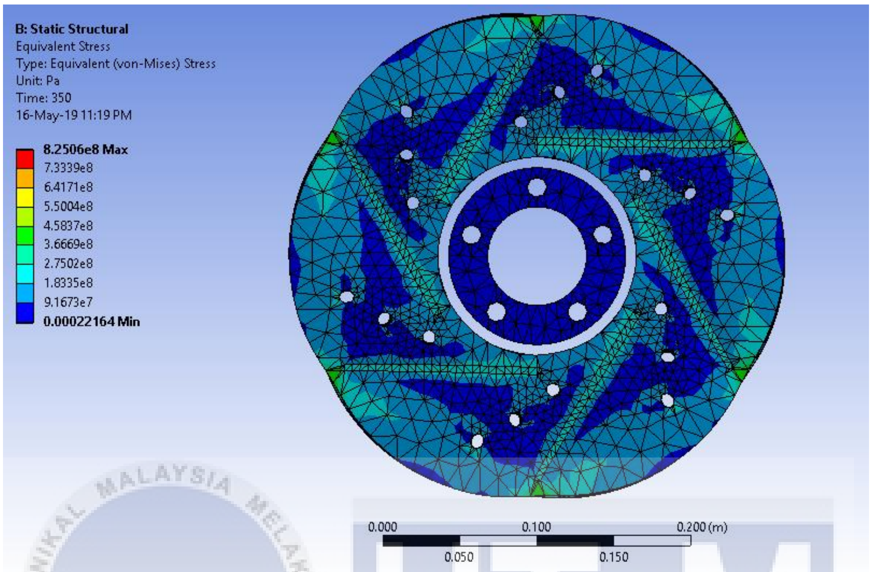

Figure 5.21: Equivalent (Von-Mises) stress of slotted and drilled rotor in static structure analysis

5.1.4 Transient Structure Analysis

The maximum and minimum deformation of blank rotor in transient structure analysis is 0.0005838 m and 0.0000030142 m. Figure 5.22 shows the total deformation of blank rotor in transient structure analysis.

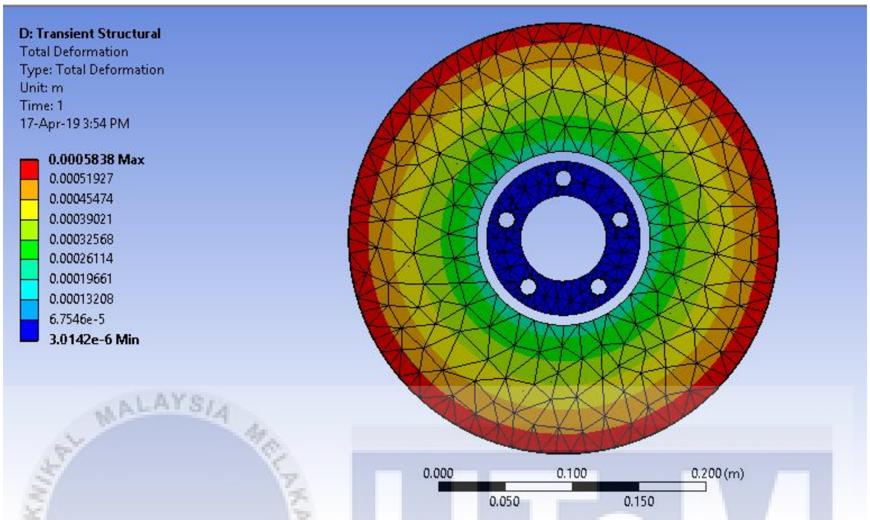

Figure 5.22: Total deformation of blank rotor in transient structure analysis

The maximum and minimum equivalent (Von-Mises) stress for blank rotor in transient structure analysis is 71.448 MPa and 0.013181 Pa. Figure 5.23 shows the equivalent (Von-Mises) stress of blank rotor in transient structure analysis.

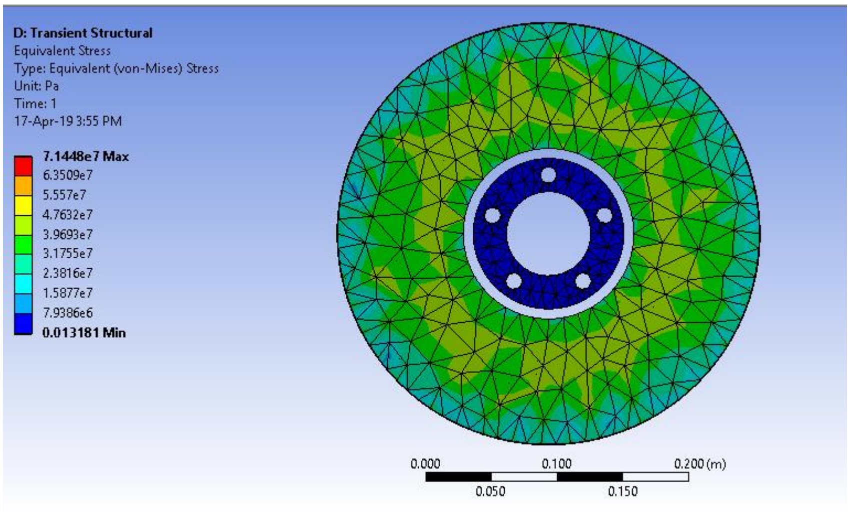

Figure 5.23: Equivalent (Von-Mises) stress of blank rotor in transient structure analysis

The maximum and minimum deformation of drilled rotor in transient structure analysis is 0.00051083 m and 0.0000027633 m. Figure 5.24 shows the total deformation of drilled rotor in transient structure analysis.

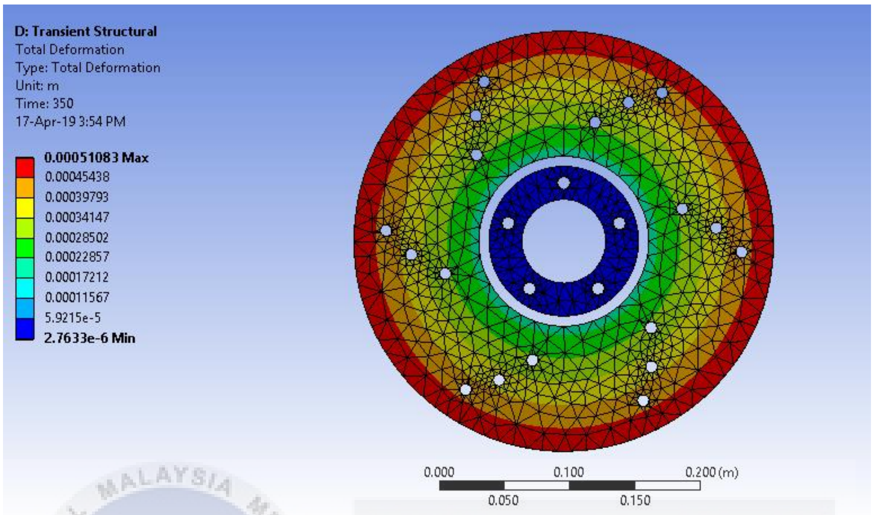

Figure 5.24: Total deformation of drilled rotor in transient structure analysis

The maximum and minimum equivalent (Von-Mises) stress for drilled rotor in transient structure analysis is 33.673 MPa and 0.016663 Pa. Figure 5.25 shows the equivalent (Von-Mises) stress of drilled rotor in transient structure analysis.

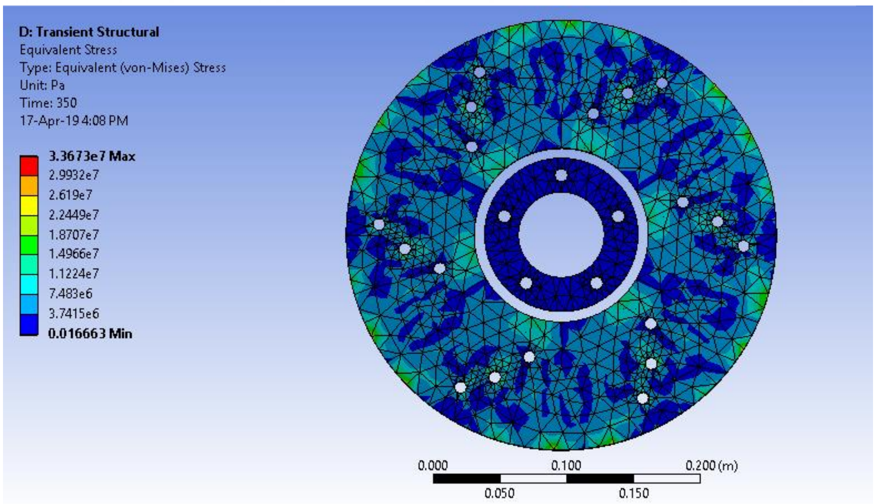

Figure 5.25: Equivalent (Von-Mises) stress of drilled rotor in transient structure analysis

The maximum and minimum deformation of slotted rotor in transient structure analysis is 0.00024317 m and 0.000002763 m. Figure 5.26 shows the total deformation of slotted rotor in transient structure analysis.

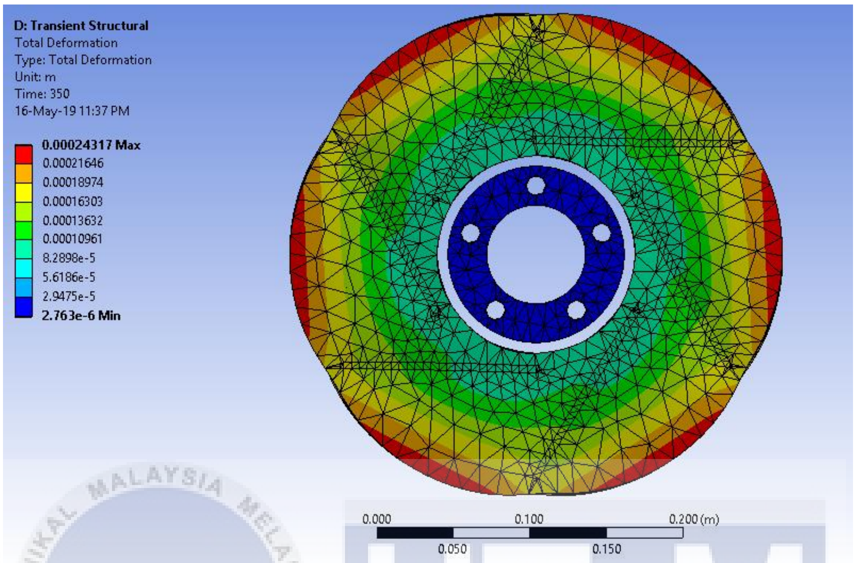

Figure 5.26: Total deformation of slotted rotor in transient structure analysis

The maximum and minimum equivalent (Von-Mises) stress for slotted rotor in transient structure analysis is 235.95 MPa and 0.0031542 Pa. Figure 5.27 shows the equivalent (Von-Mises) stress of slotted rotor in transient structure analysis.

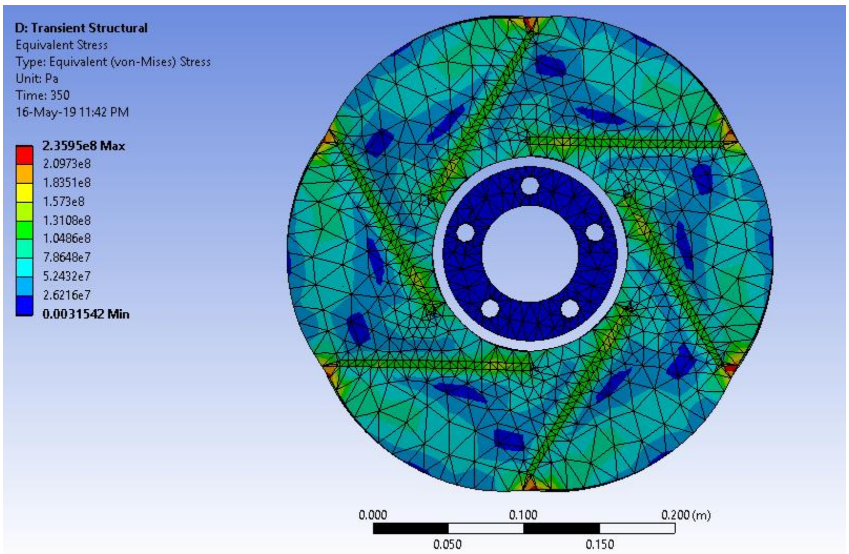

Figure 5.27: Equivalent (Von-Mises) stress of slotted rotor in transient structure analysis

The maximum and minimum deformation of slotted and drilled rotor in transient structure analysis is 0.000240777 *m* and 0.000002463 *m*. Figure 5.28 shows the total deformation of slotted and drilled rotor in transient structure analysis.

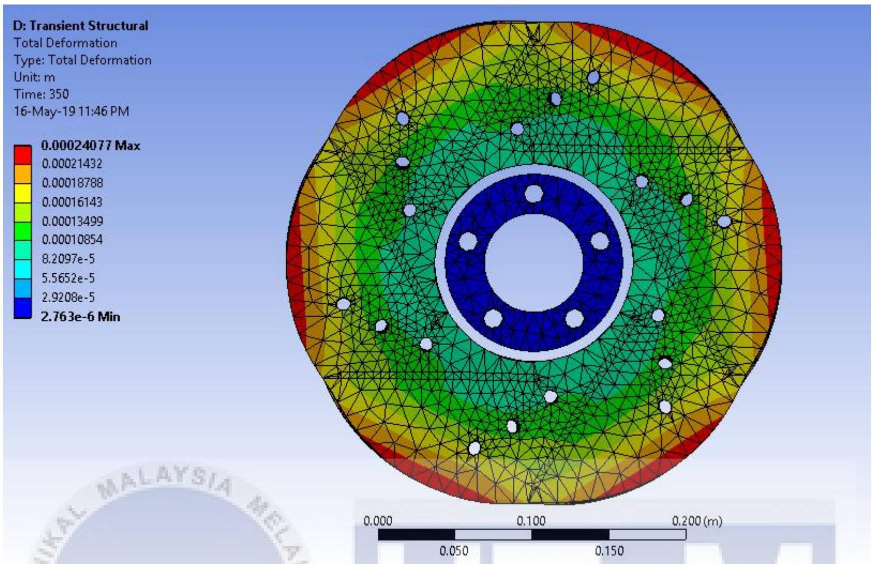

Figure 5.28: Total deformation of slotted and drilled rotor in transient structure analysis

The maximum and minimum equivalent (Von-Mises) stress for slotted and drilled rotor in transient structure analysis is $469.62\ MPa$ and $0.000016072\ Pa$. Figure 5.29 shows the equivalent (Von-Mises) stress of slotted and drilled rotor in transient structure analysis.

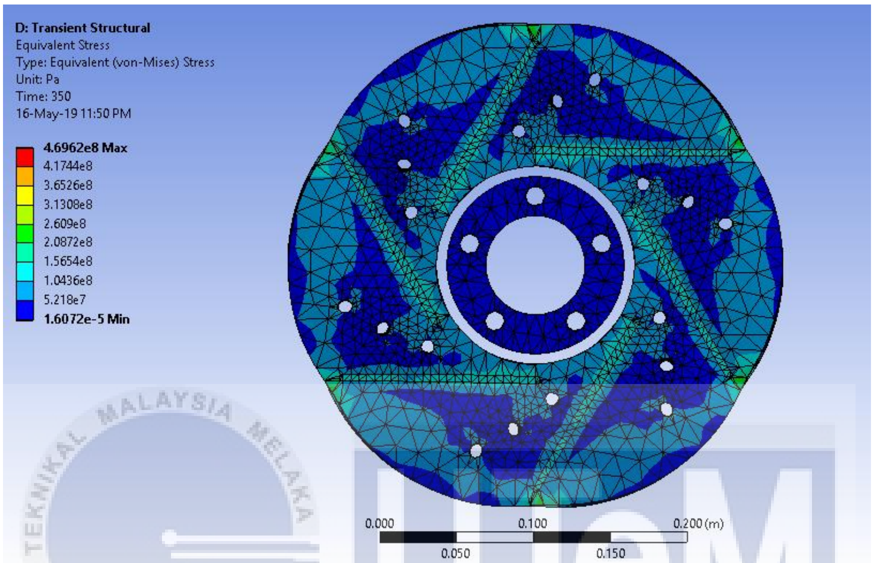

Figure 5.29: Equivalent (Von-Mises) stress of slotted and drilled rotor in transient structure analysis

5.2 Discussion

Table 5.1 and 5.2 shows the summary of the result. In steady state thermal analysis, a constant heat flux is applied to the annular ring surface of each rotor for 350 *s*. The convective heat transfer coefficient of each surface is applied from 0 *s* to 350 *s*. The slotted and drilled rotor shows a lowest temperature of 551.74 *K* compared to blank rotor (981.12 *K*), drilled rotor (969.32 *K*), and slotted rotor (803.27 *K*). It is because the slotted and drilled rotor has a larger surface to dissipate the heat. This geometry creates an additional flow across the external area especially the slotted area.

In transient thermal analysis, 10 load cycle with total time 350 seconds are applied to determine the temperature of disc brake. Each cycle consists of 6 seconds of heating and 29 seconds of cooling. A constant heat flux is applied to the annular ring surface for 6 seconds and there will be no heat flux for remaining 29 seconds. The convective heat transfer coefficient of each surface is applied from 0 *s* to 350 *s*. The slotted and drilled rotor shows a lowest temperature of 551.74 *K* compared to blank rotor (651.57 *K*), drilled rotor (635.80 *K*), and slotted rotor (552.68 *K*). This result is similar to the steady state thermal analysis. The additional surface creates an external flow to dissipate the heat through convection.

In static structure analysis, the result of steady state thermal analysis is applied to the static structure analysis. The slotted and drilled rotor shows a lowest deformation of 0.45927 *mm* compared to the blank rotor (1.04810 *mm*), drilled rotor (1.01440 *mm*), and slotted rotor (0.46808 *mm*). However, the slotted and drilled rotor shows the highest equivalent (Von-Mises) stress of 825.06 *MPa* compared to blank rotor (713.49 *MPa*), drilled rotor (575.66 *MPa*), and slotted rotor (469.23 *MPa*).

In transient structure analysis, the result of transient thermal analysis is applied to the transient structure analysis. The slotted and drilled rotor shows a lowest deformation of 0.240777 *m* compared to blank rotor (0.583800 *m*), drilled rotor (0.510830 *m*), and slotted rotor (0.243170 *m*). However, the slotted and drilled rotor shows the highest equivalent (Von-Mises) stress of 469.620 *MPa* compared to blank rotor (71.448 *MPa*), drilled rotor (33.673 *MPa*), and slotted rotor (469.620 *MPa*).

Table 5.1: Summary of result (Maximum)

Type of rotor		**Blank Rotor**	**Drilled rotor**	**Slotted rotor**	**Slotted and drilled rotor**
		Maximum	**Maximum**	**Maximum**	**Maximum**
Steady state thermal analysis	**Temperature, *K***	981.12	969.32	803.27	801.86
Transient thermal analysis	**Temperature, *K***	651.57	635.80	552.68	551.74
Static structure analysis	**Total deformation, *mm***	1.04810	1.01440	0.46808	0.45927
	Equivalent (Von-Mises) stress, *Pa*	713.49 *M*	575.66 *M*	469.23 *M*	825.06 *M*
Transient structure analysis	**Total deformation, *mm***	0.583800	0.510830	0.243170	0.240777
	Equivalent (Von-Mises) stress, *Pa*	71.448 *M*	33.673 *M*	235.950 *M*	469.620 *M*

Figure 5.30, 5.31, and 5.32 show the graph of maximum temperature, maximum total deformation, and maximum equivalent (Von-Mises) stress versus type of analysis.

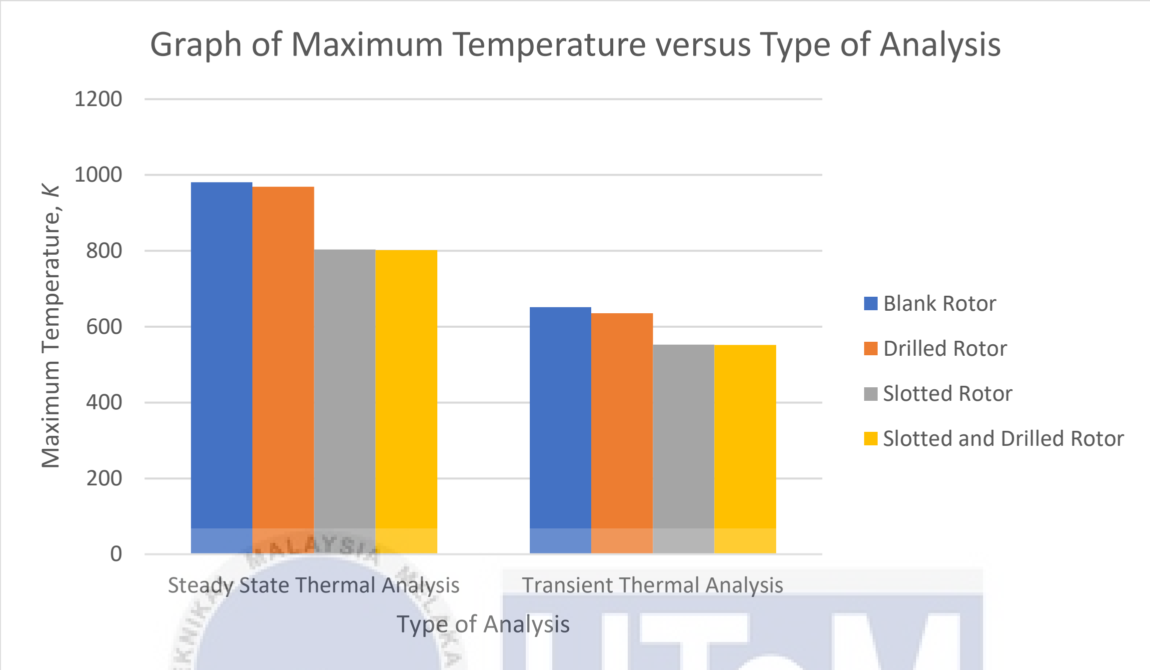

Figure 5.30: Graph of maximum temperature versus type of analysis

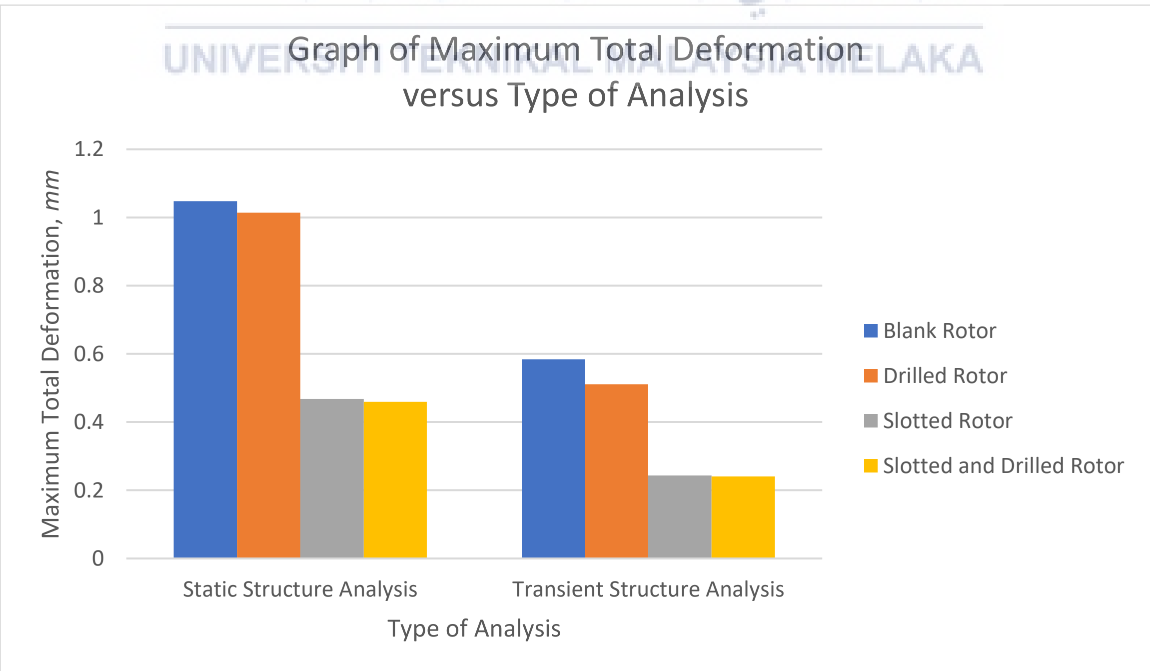

Figure 5.31: Graph of maximum total deformation versus type of analysis

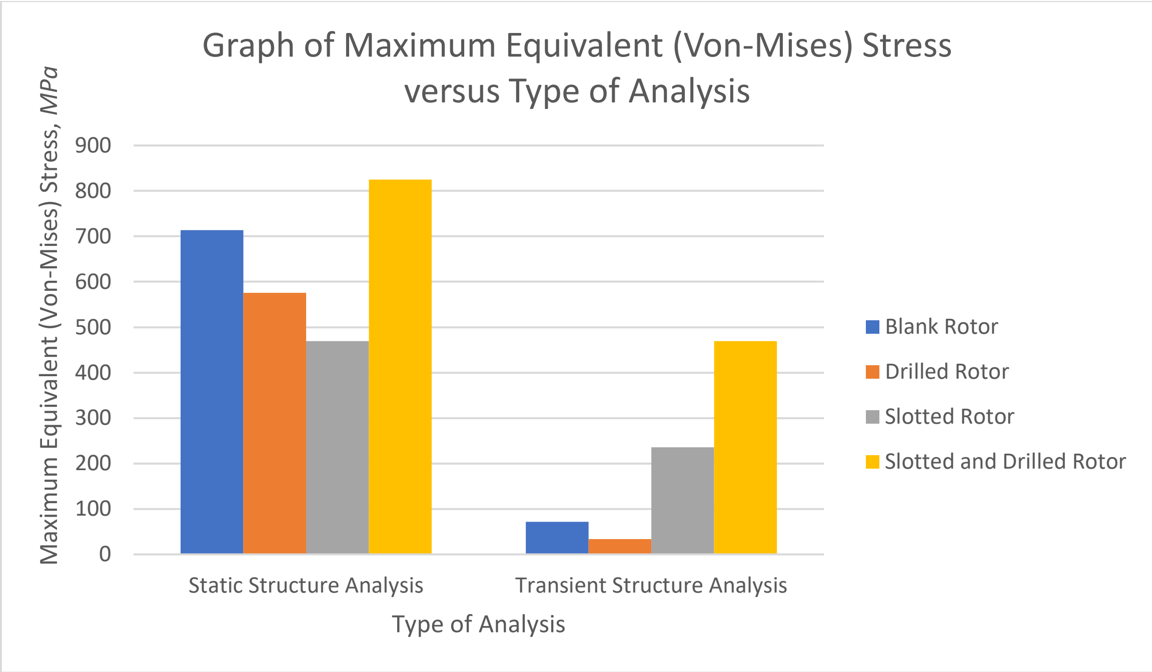

Figure 5.32: Graph of maximum equivalent (Von-Mises) stress versus type of analysis

Table 5.2: Summary of result (Minimum)

Type of rotor		**Blank Rotor**	**Drilled rotor**	**Slotted rotor**	**Slotted and drilled rotor**
		Minimum	**Minimum**	**Minimum**	**Minimum**
Steady state thermal analysis	**Temperature, *K***	480.17	470.78	303.00	302.03
Transient thermal analysis	**Temperature, *K***	303.00	303.00	303.00	300.85
Static structure analysis	**Total deformation, *mm***	0.1974700	0.1856700	0.0027629	0.0027298
	Equivalent (Von-Mises) stress, *Pa*	1560000.00	741210.00	0.00018872	0.00022164
Transient structure analysis	**Total deformation, *mm***	0.00301420	0.00276330	0.00276300	0.00246300
	Equivalent (Von-Mises) stress, *Pa*	0.013181000	0.016663000	0.003154200	0.000016072

Figure 5.33, 5.34, and 5.35 show the graph of maximum temperature, maximum total deformation, and maximum equivalent (Von-Mises) stress versus type of analysis.

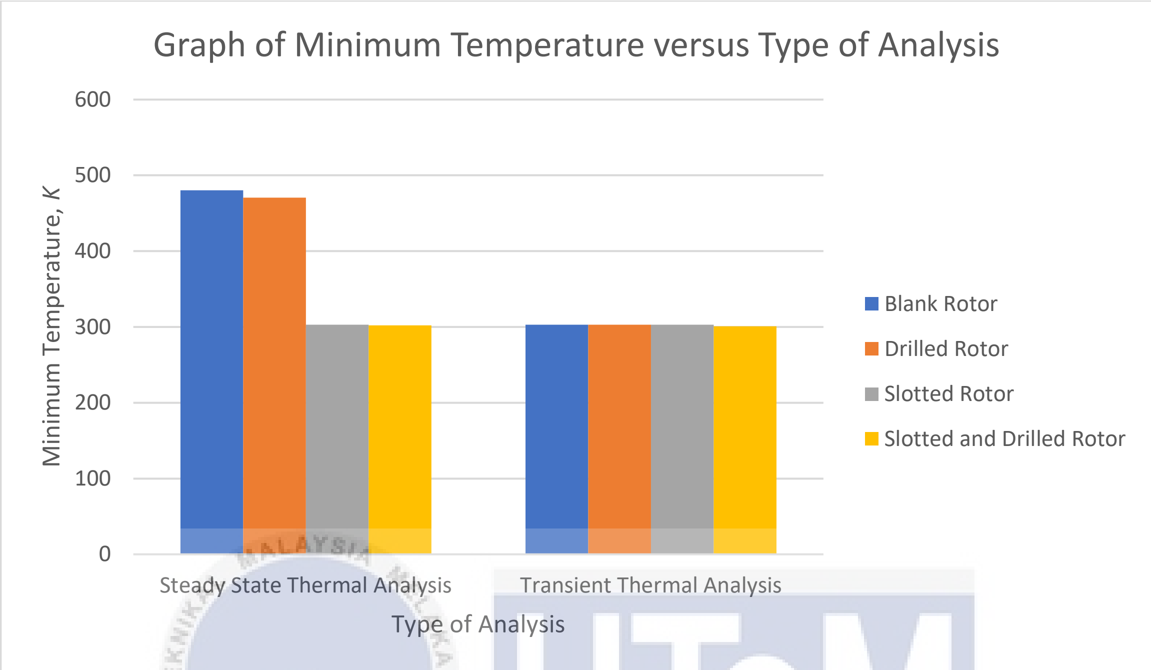

Figure 5.33: Graph of minimum temperature versus type of analysis

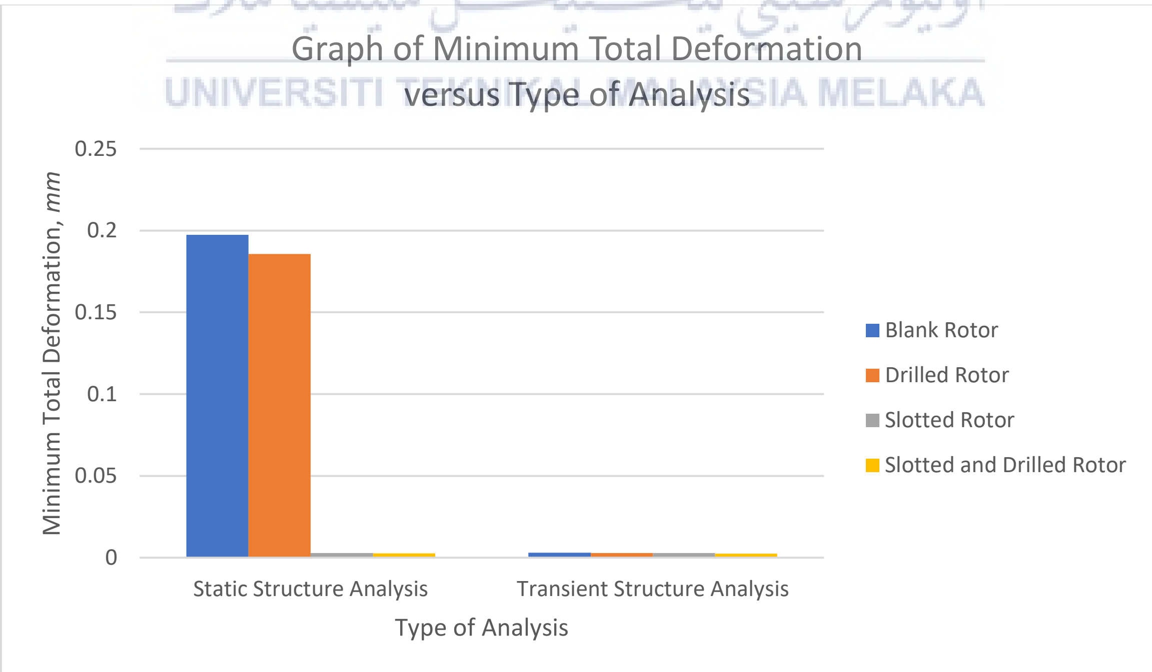

Figure 5.34: Graph of minimum total deformation versus type of analysis

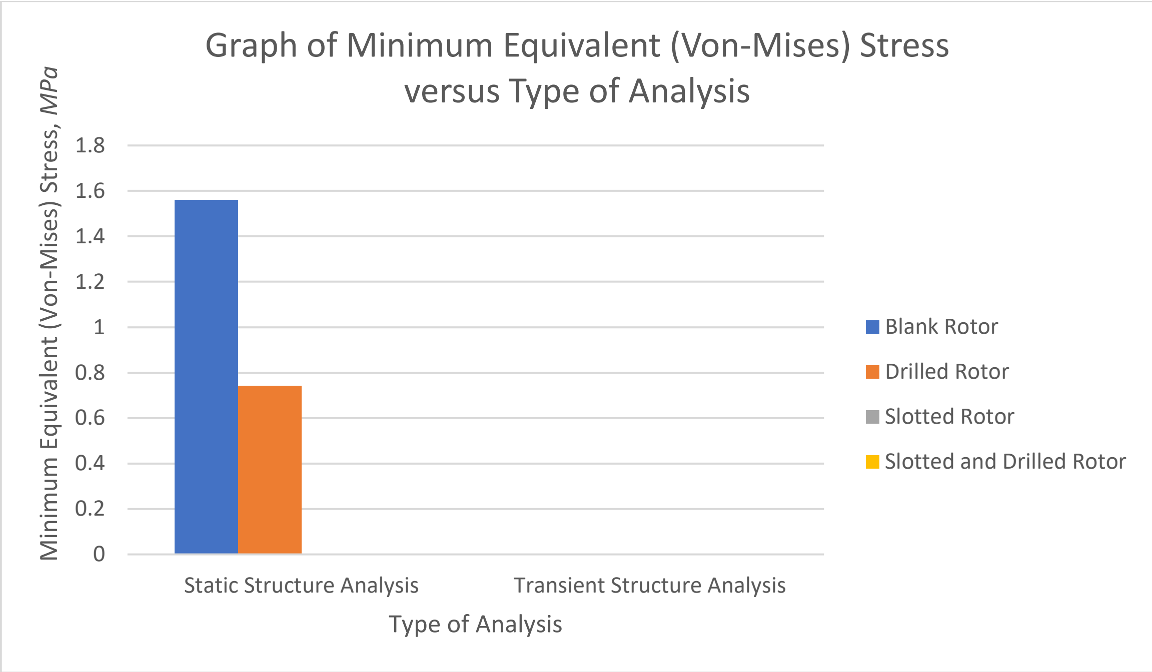

Figure 5.35: Graph of minimum equivalent (Von-Mises) stress versus type of analysis

5.3 Validation of Result

During the repeated braking operation, the disc is treated as a lumped system. The thermal properties and heat transfer coefficient are constant. The temperature of the rotor is assumed to be uniform across the rotor (Limpert 2011). Eq. (5.1) is used when the braking time is considerably less the cooling time while ΔT is the average temperature increase per stop. In this case, the braking time for one cycle is 6 s and cooling time is 29 s.

$$\Delta T = \frac{P_b t_s}{p_R c_R V_R} \tag{5.1}$$

Braking power absorbed by the rotor, P_R = $1(1632)(6.11)(30.56) = 304785\ W$

Time to stop, t_s = 6 s

Density of rotor, p_R = 7200 kgm^{-3}

Specific heat of rotor, C_R = 586 $Jkg^{-1}K^{-1}$

Volume of rotor, V_R = 0.001 m^3

$$\Delta T = \frac{304785 \times 6}{7200 \times 586 \times 0.001} = 433.4\ K$$

According to Limpert (2011), the Eq. (5.2) is used to calculate the temperature after a cycle of braking and cooling while T_n is the temperature after *n th* brake application.

$$T_n - T_\infty = \frac{\left[1-e^{\frac{-n_a h_R A_R t_c}{p_R C_R V_R}}\right][\Delta T]}{[1-e^{\frac{-h_R A_R t_c}{p_R C_R V_R}}]} \tag{5.2}$$

Number of brake application, $-n_a$ = $1, 2, 3, 4, 5, 6, 7, 8, 9, 10$

Heat transfer coefficient, h_R = $230.5\ Wm^{-2}K^{-1}$

Area of rotor surface, A_R = $0.1044\ m^2$

Total time, t_c = $350\ s$

Density of rotor, p_R = $7200\ kgm^{-3}$

Specific heat of rotor, C_R = $586\ Jkg^{-1}K^{-1}$

Volume of rotor, V_R = $0.001\ m^3$

Surrounding temperature, T_∞ = $303\ K$

The temperature after 1 load cycle is recorded. Table 5.3 shows the result of ANSYS and result of Eq. (5.2). The magnitude of temperature that calculated using the Eq. (5.2) shows a higher temperature compared to the result of ANSYS. However, both of the result shows a constant temperature after 6 load cycle is applied to the rotor.

Table 5.3: Result of ANSYS and Eq. (5.2)

Load cycle	**Result of ANSYS**	**Result of calculation (Limpert, 2011)**
0	303.00	303.00
1	542.50	719.14
2	622.84	775.67
3	658.81	783.35
4	674.95	784.39
5	682.19	784.53
6	685.43	784.55
7	686.89	784.56
8	687.54	784.56
9	687.84	784.56
10	651.57	784.56

Figure 5.36 shows the comparison of validation result. The blue line indicates the result of manual calculation and the red line indicates the result of ANSYS. Both of the result shows a constant temperature after it reach a certain temperature. This is because the rate of heat dissipate by the convection is increasing and it is directly proportional to the rotational speed of rotor. The higher the velocity of vehicle, the higher the rate of heat dissipate by convection. The percentage different of both results is about 15~20 %. Therefore, the result is accepted.

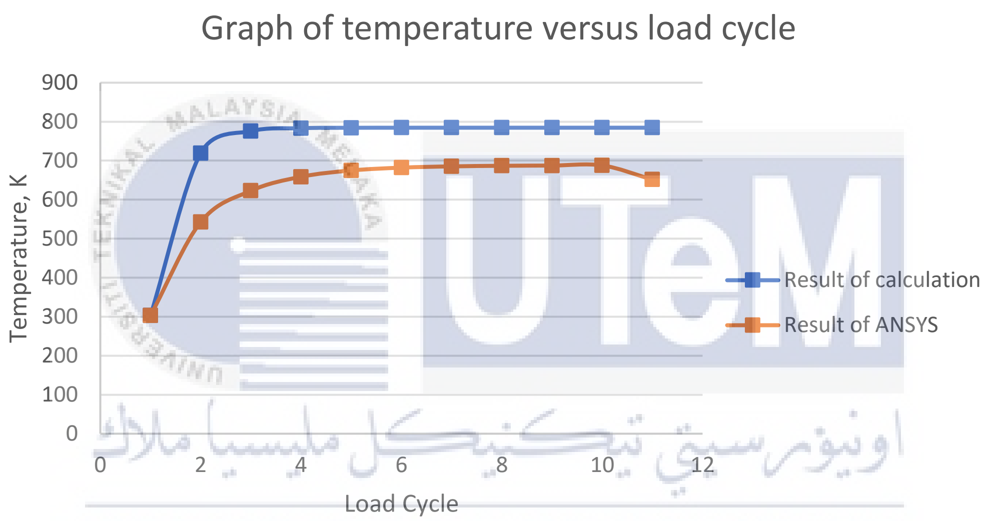

Figure 5.36: Comparison of validation result

CHAPTER 6

CONCLUSION AND RECOMMENDATON

6.1 Conclusion

In this project, a literature study about the relating theory is completed. The information such as trend of industry, working principle, specification of rotor, type of brake pad, mode of heat transfer, and theory of FEA is explained in the literature review. Four ventilated disc brake rotor with different design specification is selected as the object of this project, which is blank rotor, drilled rotor, slotted rotor, and slotted and drilled rotor. The 3D model is designed by using SolidWorks. The technical specification of vehicle and dimension of disc brake rotor is defined and recorded from the online shop. The calculation of convective heat transfer coefficient for certain surface that exposed to the air is completed. After that, the value for each calculation is inserted into ANSYS for steady state thermal analysis, transient thermal analysis, static structure analysis and transient structure analysis.

Due to the conduction and radiation are ignored in this project, the actual temperature could be less than the temperature of analysis. Furthermore, the convection is the most efficient mode of heat transfer at the higher speed compared to conduction and radiation. Thus, it is important to study the effect of design that can affect the rate of heat dissipate by convection after high speed braking operation. In conclusion, thermal stress analysis on four different design specification of cast iron rotor after several braking operation of vehicle is completed.

The convective heat transfer coefficient of slotted area is much higher compared the convective heat transfer coefficient of another surface. Therefore, the slotted rotor shows a lower temperature in steady state thermal analysis and transient thermal analysis compared to another rotors. Furthermore, the slotted rotor shows a lower deformation and moderate equivalent (Von-Mises) stress in static structure analysis and transient structure analysis.

6.2 Recommendation

The slotted and drilled rotor shows a lowest temperature in steady state thermal analysis (801.86 *K*) and transient thermal analysis (551.74 *K*). Moreover, the slotted and drilled rotor shows a lowest deformation in static structure analysis (0.45927 *m*) and transient structure analysis (0.240777 *m*). However, the slotted rotor and drilled rotor shows a highest equivalent (Von-Mises) stress in static structure analysis (825.06 *MPa*) and transient structure analysis (469.62 *MPa*). Therefore, slotted and drilled rotor has a result of lowest temperature, lowest deformation and highest equivalent (Von-Mises) stress.

The slotted rotor shows a higher temperature of 803.27 *K* in steady state thermal analysis and 552.68 *K* in transient thermal analysis compared to slotted and drilled rotor. The difference between the result of both rotors are 1.41 *K* in steady state thermal analysis and 0.94 *K* in transient thermal analysis. The deformation of slotted rotor is slightly higher than the deformation of slotted and drilled rotor. The slotted rotor shows a deformation of 0.46808 *mm* in static structure analysis and 0.24317 *mm* in transient structure analysis. The difference between the result of both rotors are 0.00881 *mm* in static structure analysis and 0.002393 *mm* in transient structure analysis. The equivalent (Von-Mises) stress of slotted rotor is 469.23 *MPa* in static structure analysis and 235.95 *MPa* in transient structure analysis. It is much lower than the equivalent (Von-Mises) stress of slotted and drilled rotor. The difference of equivalent (Von-Mises) stress of both rotors is 355.83 *MPa* in static structure analysis and 233.65 *MPa* in transient structure analysis.

The slotted rotor shows a lower temperature in steady state thermal analysis and transient thermal analysis compared to blank rotor and drilled rotor. Furthermore, it shows a lower deformation in static structure analysis and transient structure analysis compared to blank rotor and drilled rotor. The equivalent (Von-Mises) stress of slotted rotor is lower than the equivalent (Von-Mises) stress of blank rotor and drilled rotor in static structure analysis. However, equivalent (Von-Mises) stress of slotted rotor is higher than the equivalent (Von-Mises) stress of blank rotor and drilled rotor in transient structure analysis.

In term of sustainable development, the lifespan of slotted and drilled rotor will be shorter than the lifespan of blank rotor, drilled rotor, and slotted rotor. It is because the equivalent (Von-Mises) stress of slotted and drilled rotor is much bigger compared to blank rotor, drilled rotor, and slotted rotor. Therefore, the slotted rotor is the best rotor compared to blank rotor, drilled rotor, and slotted and drilled rotor.

REFERENCES

Amrish P. N. (2016) 'Computer Aided Design and Analysis of Disc Brake Rotors', *Advances in Automobile Engineering*, 05(02). doi: 10.4172/2167-7670.1000144.

Automotive Mechanics,2E - S. Srinivasan - Google book. 2nd Editio (2003). Tata McGraw-Hill Publishing Company. Available at: https://books.google.com.my/books?id=1zmaSZRhAroC&printsec=frontcover&hl=zh-CN&source=gbs_ge_summary_r&cad=0#v=onepage&q&f=false (Accessed: 27 November 2018).

Belhocine A., Abu Bakar A. R., and Bouchetara M. (2016) 'Thermal and structural analysis of disc brake assembly during single stop braking event', *Australian Journal of Mechanical Engineering*. Taylor & Francis, 14(1), pp. 26–38. doi: 10.1080/14484846.2015.1093213.

Complete Guide to Disc Brakes and Drum Brakes - Les Schwab (no date). Available at: https://www.lesschwab.com/article/complete-guide-to-disc-brakes-and-drum-brakes.html (Accessed: 27 November 2018).

Deshpand, S. and Kamat A. (2017) 'Review on Thermal Cracking Phenomenone in Brake Disc', 6(06), pp. 233–237.

Greibe P. (2007) 'Braking distance , friction and behaviour', (July).

Vikas Gupta, Kuldeep Saini, Ashok Kumar Garg, Gopal Krishan, and Om Parkash (2016) 'Comparative Analysis of Disc Brake Model for Different Materials Investigated Under Tragic Situations', 5(1), pp. 18–23.

Hingu, V. H. (2017) 'Thermal Analysis on Disc Brakes Rotor', (3), pp. 267–273.

Honda (2018) *2018 Honda Civic - Owner's Manual*.

Ansys Advantage (2009) 'Excellence in engineering simulation', III(2).

Jayasudha K., Hemanth M., Baswa Raj., Raghuveer H.P., Vedavathi B., Hegde, and Chatura (2015) 'Traumatic impact loading on human maxillary incisor: A Dynamic finite element analysis', *Journal of Indian Society of Pedodontics and Preventive Dentistry*, 33(4), p. 302. doi: 10.4103/0970-4388.165680.

Limpert, R. (2011) *Brake Design and Safely*. Third Edit. Warrendale, PA USA: Society of Automotive Engineer, Inc.

Macužić. S, Saveljić S., Lukić I., Glišović J., and Filipović J. (2015) 'Thermal analysis of solid and vented disc brake during the braking process', *Journal of the Serbian Society for Computational Mechanics*, 9(2), pp. 19–26. doi: 10.5937/jsscm1502019M.

Ogunkah, I. and Yang, J. (2012) *Investigating Factors Affecting Material Selection: The Impacts on Green Vernacular Building Materials in the Design-Decision Making Process*, *Buildings*. doi: 10.3390/buildings2010001.

Satope, Sumeetn, and Akshaykumar Bote (2017) 'Thermal Analysis of Disc Brake', *International Journal for Innovative Research in Science & Technology*, 3(12), pp. 68–73.

Shahril K. S., Riduan M. I., Sabri, and M. M. S. (2014) 'Thermal Effects of Disc Brake Rotor Design for Automotive Brake Application', *International Conference on Mechanical Engineering and Applied Mechanics*.

Teertstra, P., Culham, J. R. and Yovanovich, M. M. (2014) 'Analytical Modeling of Forced Convection in Slotted Plate Fin Heat Sinks Analytical Modeling of Forced Convection in Slotted Plate Fin Heat Sinks', (March).

Tsai, Hsin-luen Teo, Han-guan Gau, Chie Jeng, S. T. Lee, C. C. Lin, S. W. Lin, and S. C. (2007) 'Transient Thermal Analysis of a Disk Brake System, Kao Yuan University , Department of Electronic Engineering National Cheng Kung University , Department of Aeronautics and Astronautics Chung Shan Institute of Science and Technology', (January

2017).

Tsukasa Azuma (2018) *Common Types of Brake Pads You Need to Know - CAR FROM JAPAN*. Available at: https://carfromjapan.com/article/car-maintenance/common-types-of-brake-pads-know/ (Accessed: 27 November 2018).

Manjunath V, TM, and Dr Suresh P (2013) 'Structural and Thermal Analysis of Disc Brake in Automobiles', *International Journal of Latest Trends in Engineering and Technology*, 2(3), pp. 18–25.

Virtual Prototyping and How It Can Benefit Your Product Design Process (no date). Available at: https://www.simscale.com/blog/2018/06/virtual-prototyping-benefit/ (Accessed: 27 November 2018).

Voller, G. P. (2003) 'Analysis of Heat Dissipation From Railway and Automotive Friction Brakes'.

APPENDIX

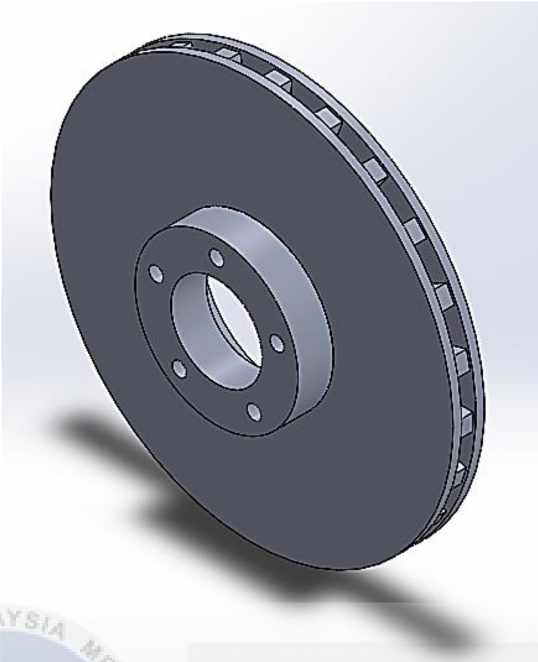

Isometric view of blank rotor

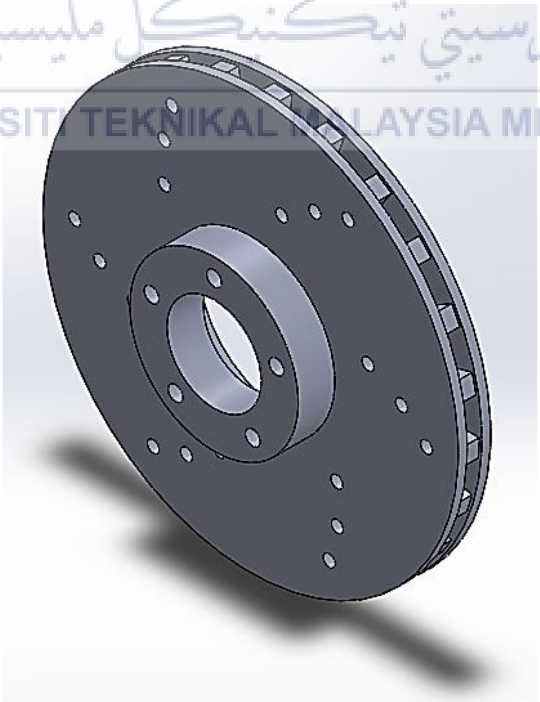

Isometric view of drilled rotor

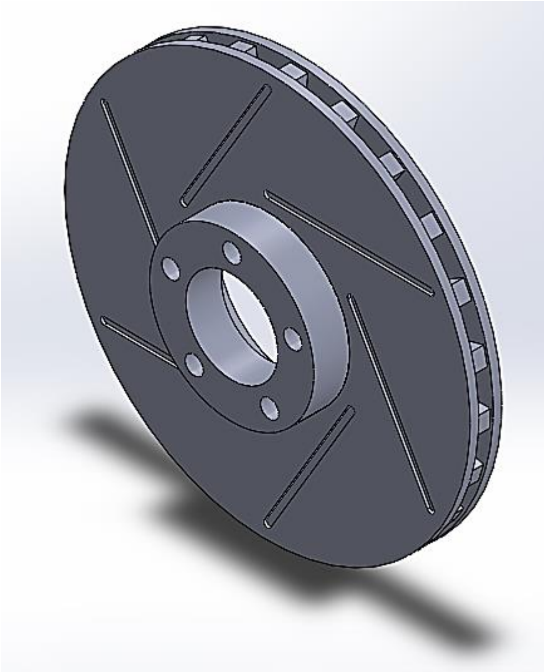

Isometric view of slotted rotor

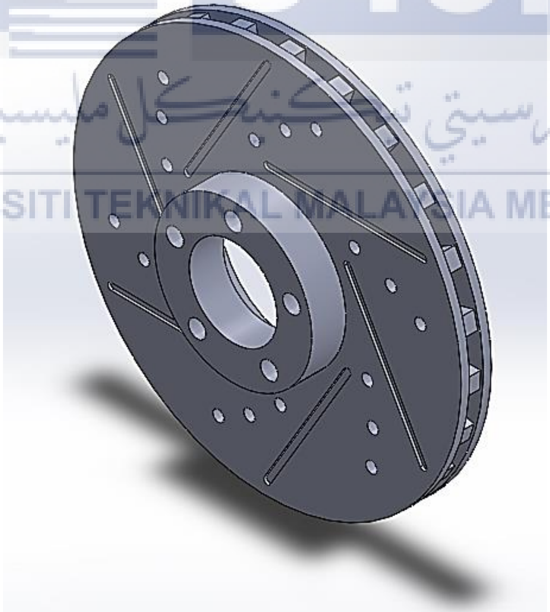

Isometric view of slotted and drilled rotor